

Single crystal neutron diffraction beyond three dimensions

Xiaoping Wang

*Neutron Scattering Division
Oak Ridge National Laboratory*

Mantid Users Workshop
ILL, Grenoble
April 3, 2019

ORNL is managed by UT-Battelle
for the US Department of Energy



Outline

- **Single crystal neutron diffraction**
 - Instrument Suite at HFIR and SNS
- **Neutron wavelength-resolved TOF Laue**
 - The concept of 3D reciprocal space mapping
- **Single crystal diffraction in $(3+n)d$ diffraction space**
 - Incommensurate charge density wave in $K_2V_3O_8$
- **Single crystal diffraction in parameter space**
 - Time filtering of event based neutron scattering data
 - Variable temperature study of structural phase transitions
 - Dynamic structural response of materials in pulsed electric field
- **Perspectives**

Single Crystal Diffraction at ORNL

<http://neutrons.ornl.gov/instruments>

HFIR

- **HB-3A DEMAND** Four-Circle Diffractometer
- **CG-4D IMAGINE** Laue Diffractometer
- **HB-2C WAND²** Wide-Angle Neutron Diffractometer

SNS

- **BL-9 CORELLI** Elastic Diffuse Scattering Spectrometer
- **BL-11B ManDi** Macromolecular Neutron Diffractometer
- **BL-12 TOPAZ** Single-Crystal Diffractometer
- **BL-3 SNAP** Spallation Neutrons and Pressure Diffractometer



Data acquisition for single crystal diffraction

Monochromatic source

- Point detector – record photon/neutron counts using a point counter
 - 1D peak integration using peak profile from step scans
- Area detector – record photon/neutron counts at 2D (x,y) pixel positions
 - 2D and 3D peak integration possible by combining frame images from step scans

White beam

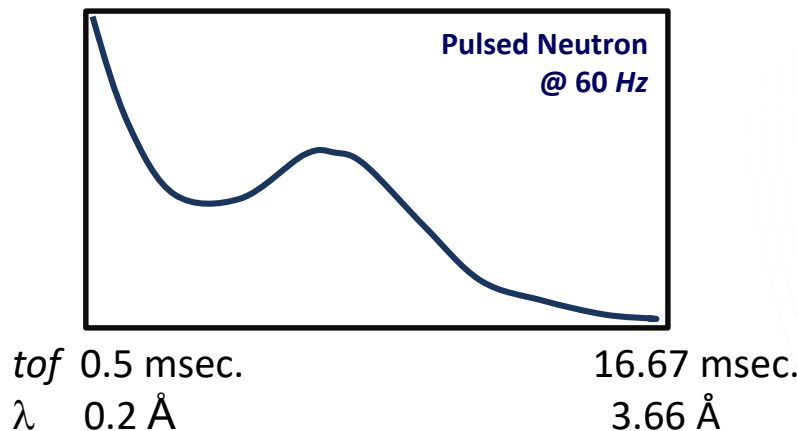
- Laue
 - [Cylindrical] Image plate – 2D (x,y) pixels
Spatial and harmonic overlap of higher order reflections
 - Quasi-Laue, limited band widths, for example, 15% in $\Delta\lambda/\lambda$
- Wavelength-resolved Laue
 - Area detectors with large Q coverage at spallation neutron sources
Neutron Time of Flight (TOF) provides wavelength resolution in 3rd dimension. **Wavelength-resolved Laue**

Neutron Time-of-Flight, TOF

- **Neutron Time of Flight:** Event based neutron detection technique
 - de Broglie equation relates neutron wavelength to its momentum:

$$\lambda = \frac{h}{mv} = \frac{h}{m} \frac{t}{L} = \frac{h}{m} \frac{t}{(L_1 + l_2)}$$

- By recording the time of a neutron arrives over a fix path length from source to detector (aka **time of flight**), its velocity, and consequently its wavelength can be measured.



Anger Camera



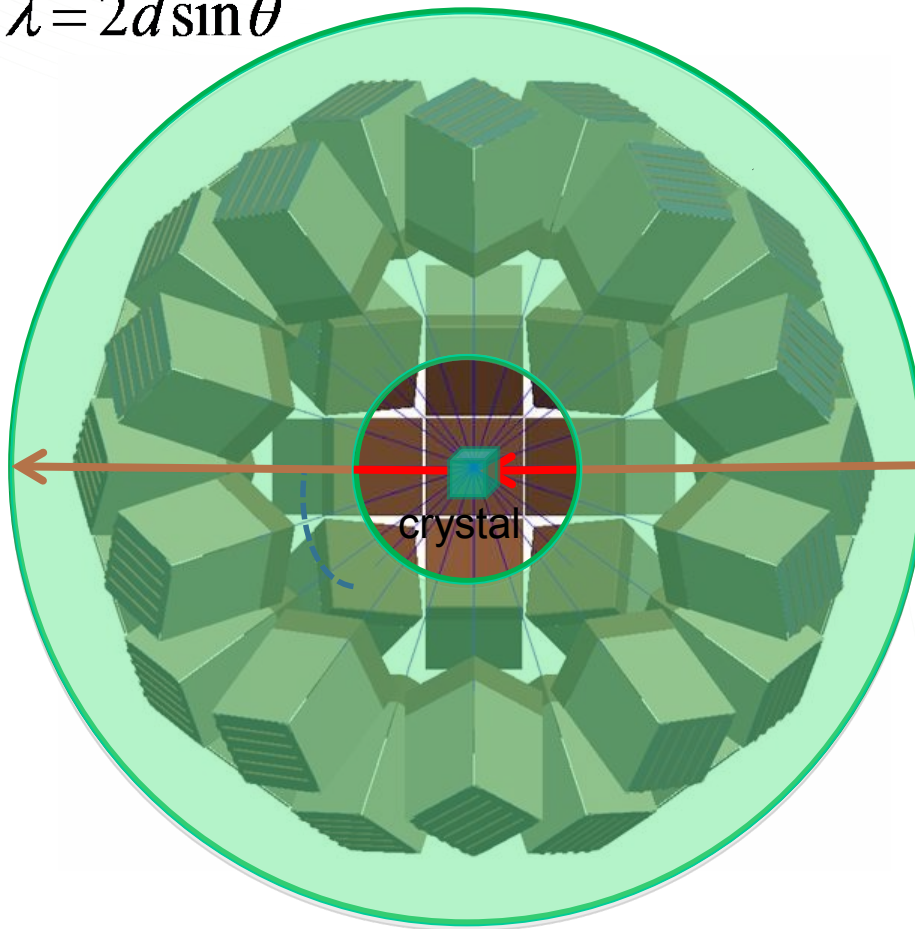
<1 μ sec readout time

Neutron Time-of-Flight Laue

Combine de Broglie's equation and Bragg's law

$$\lambda = \frac{h}{mv} = \frac{ht}{m(L_1 + l_2)}$$

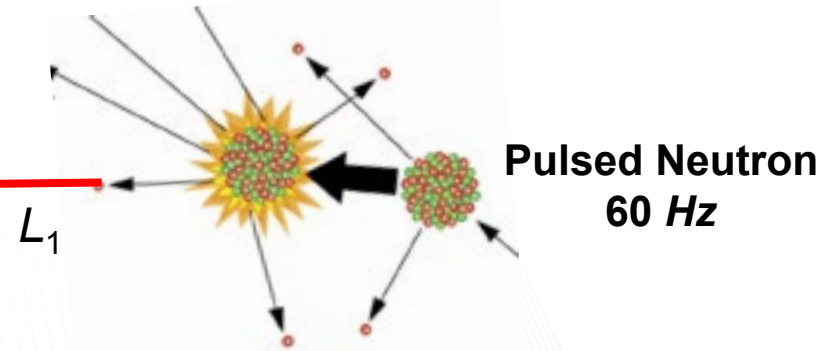
$$\lambda = 2d \sin \theta$$



$$t = \frac{m}{h} (L_1 + l_2) \times 2d \sin \theta$$

$$\begin{aligned} L_1 &= 18 \text{ m} \\ l_2 &= 0.39 \text{ to } 0.46 \text{ m} \end{aligned}$$

Neutron Time-of-flight Laue
Wavelength-resolved Laue

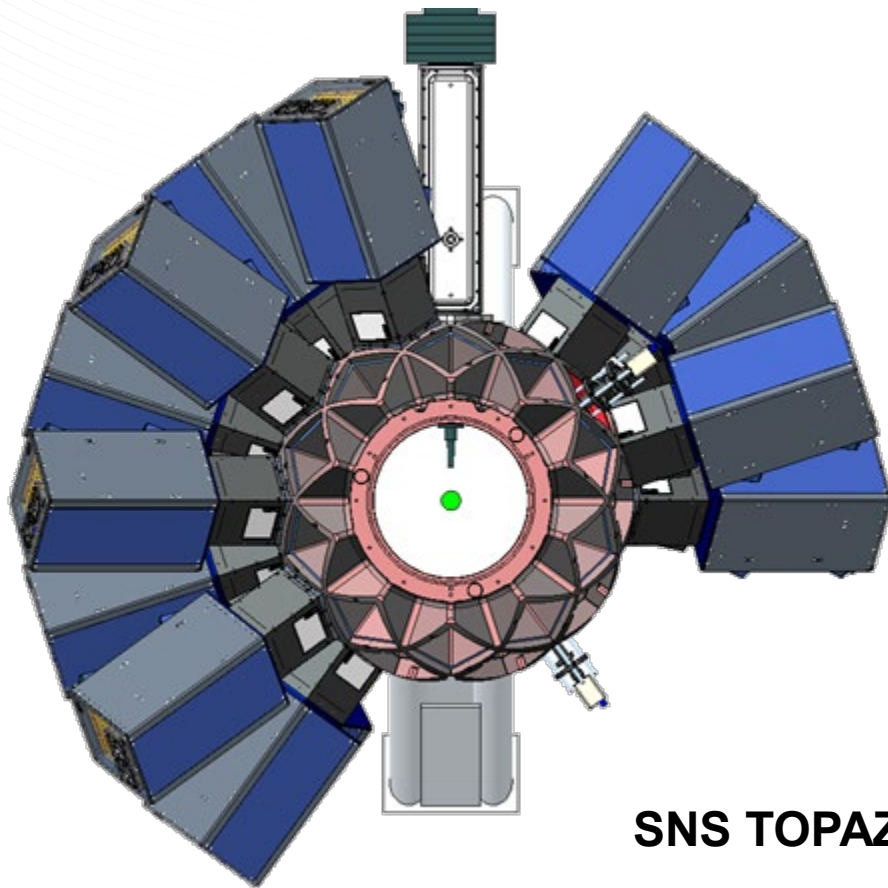


3-D Reciprocal Space Mapping

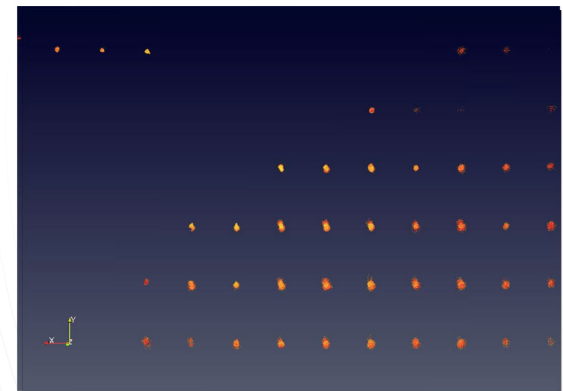
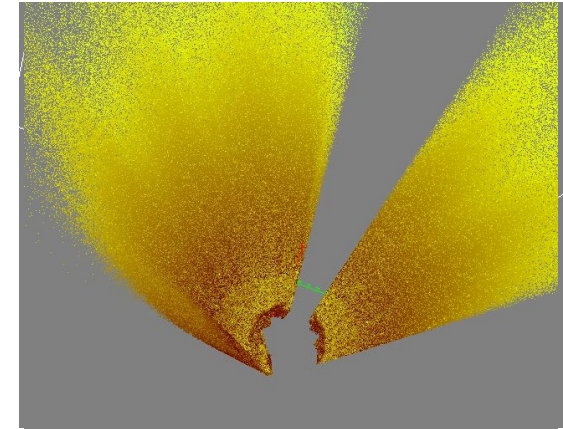
Reciprocal space mapping

3D

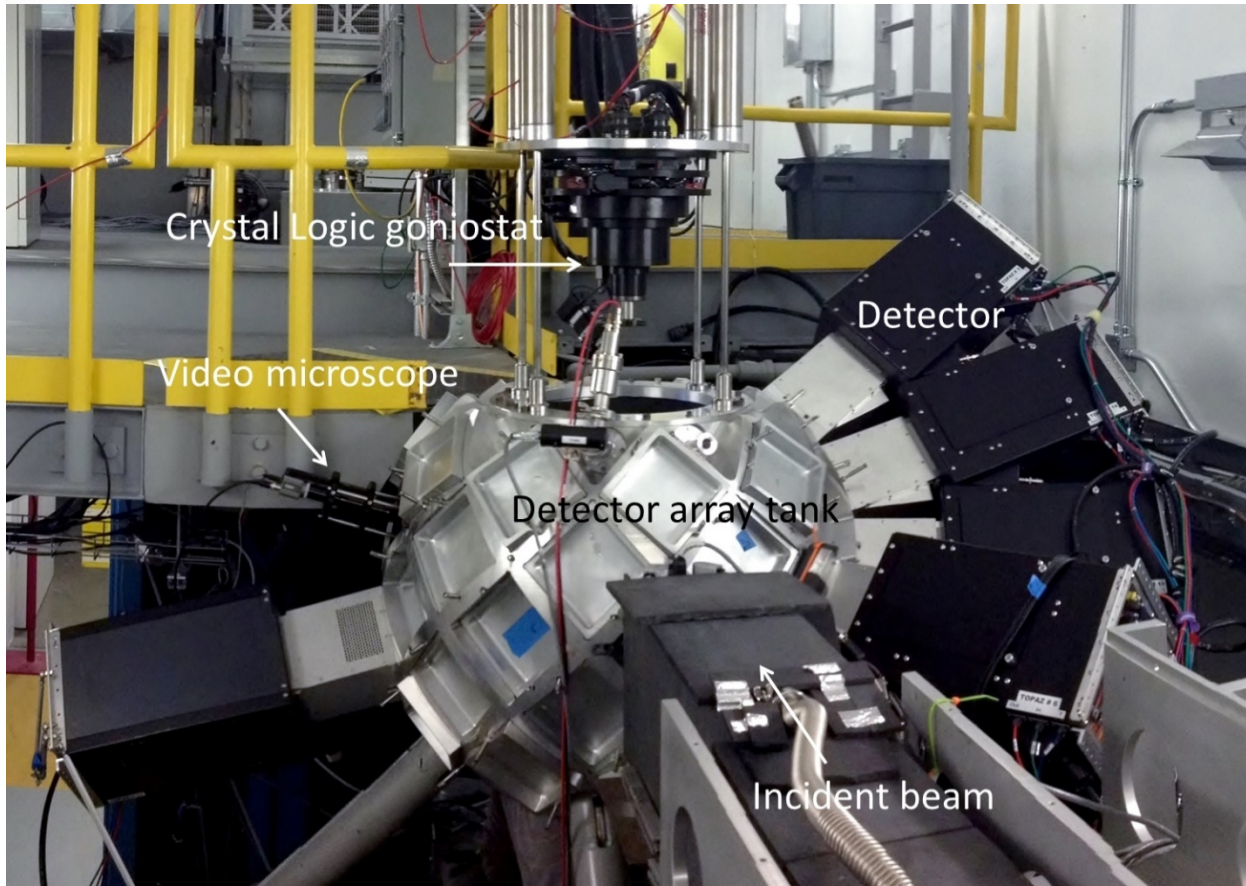
Neutron wavelength-resolved Laue



SNS TOPAZ

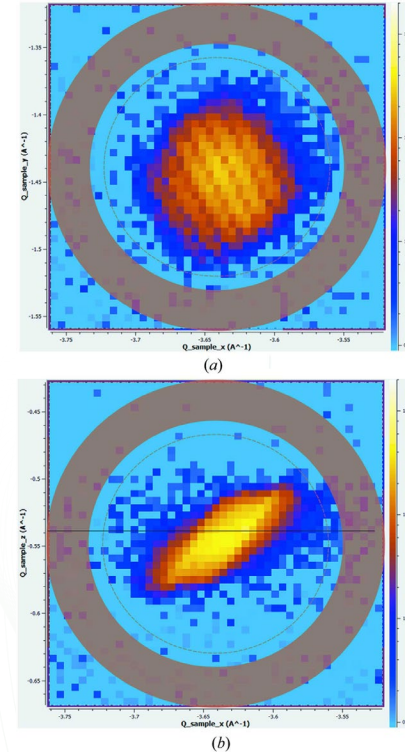
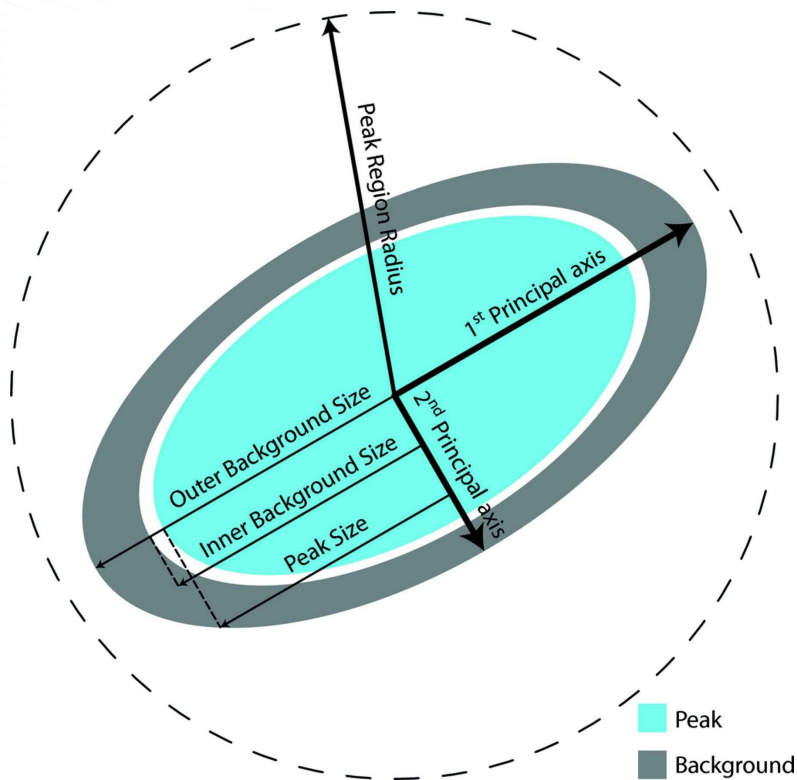


TOPAZ Single Crystal Diffractometer

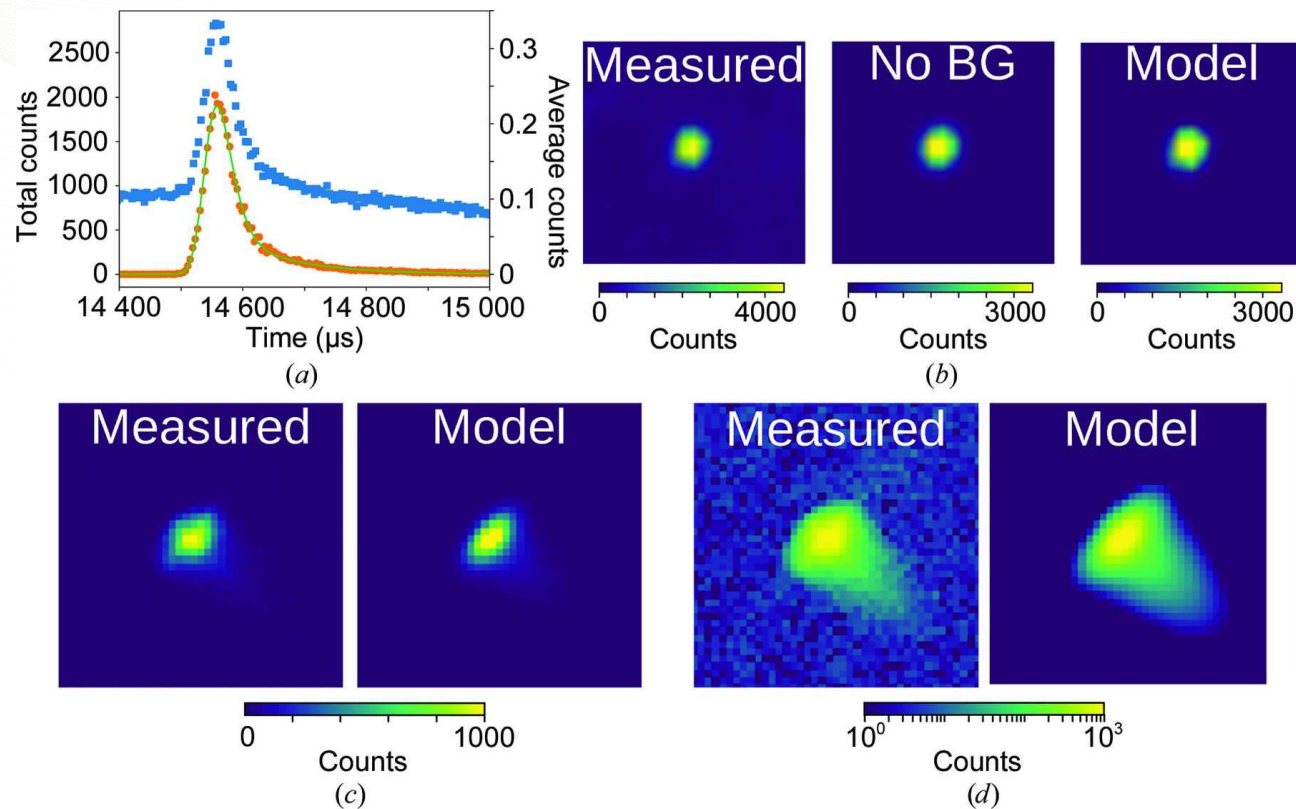


Peak integrations in 3D Q space

- Bragg peak integration using three-dimensional ellipsoids

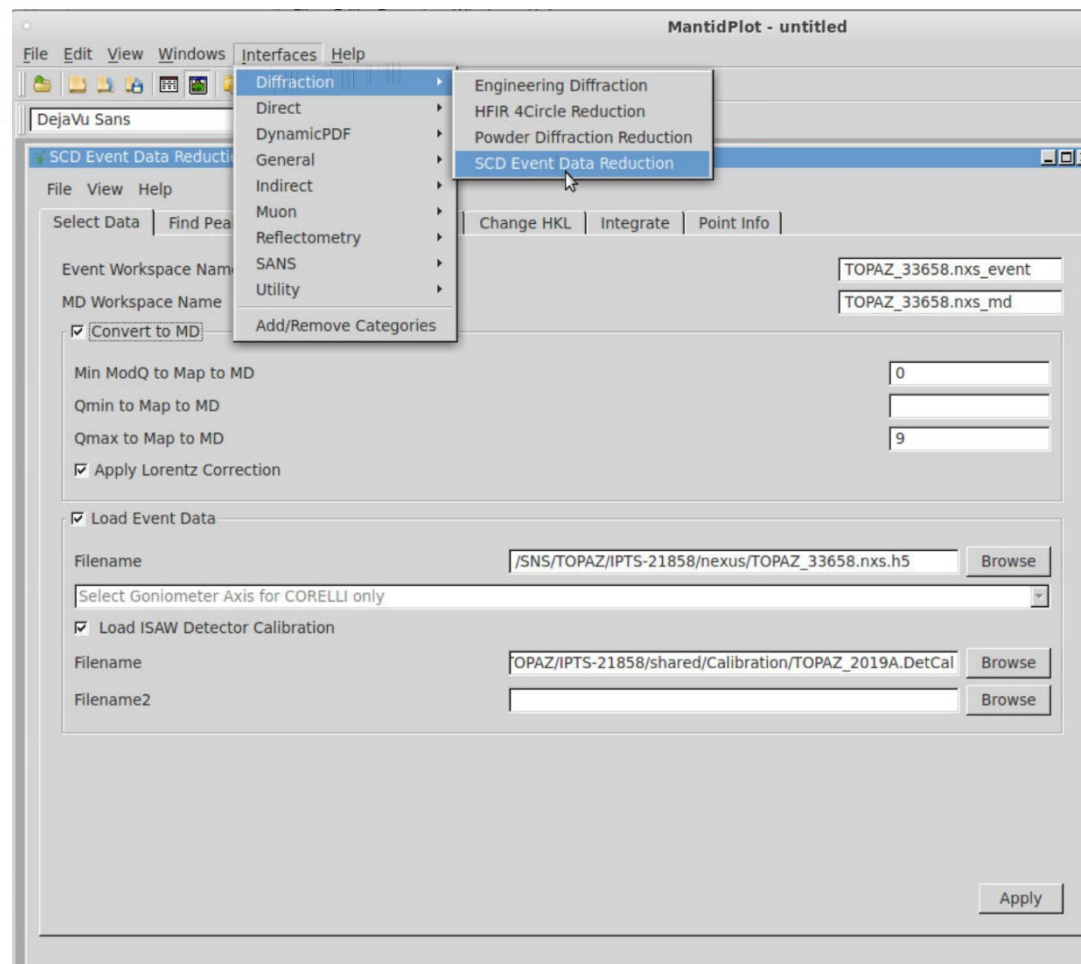


3D Profile fitting of Bragg peaks in Q space

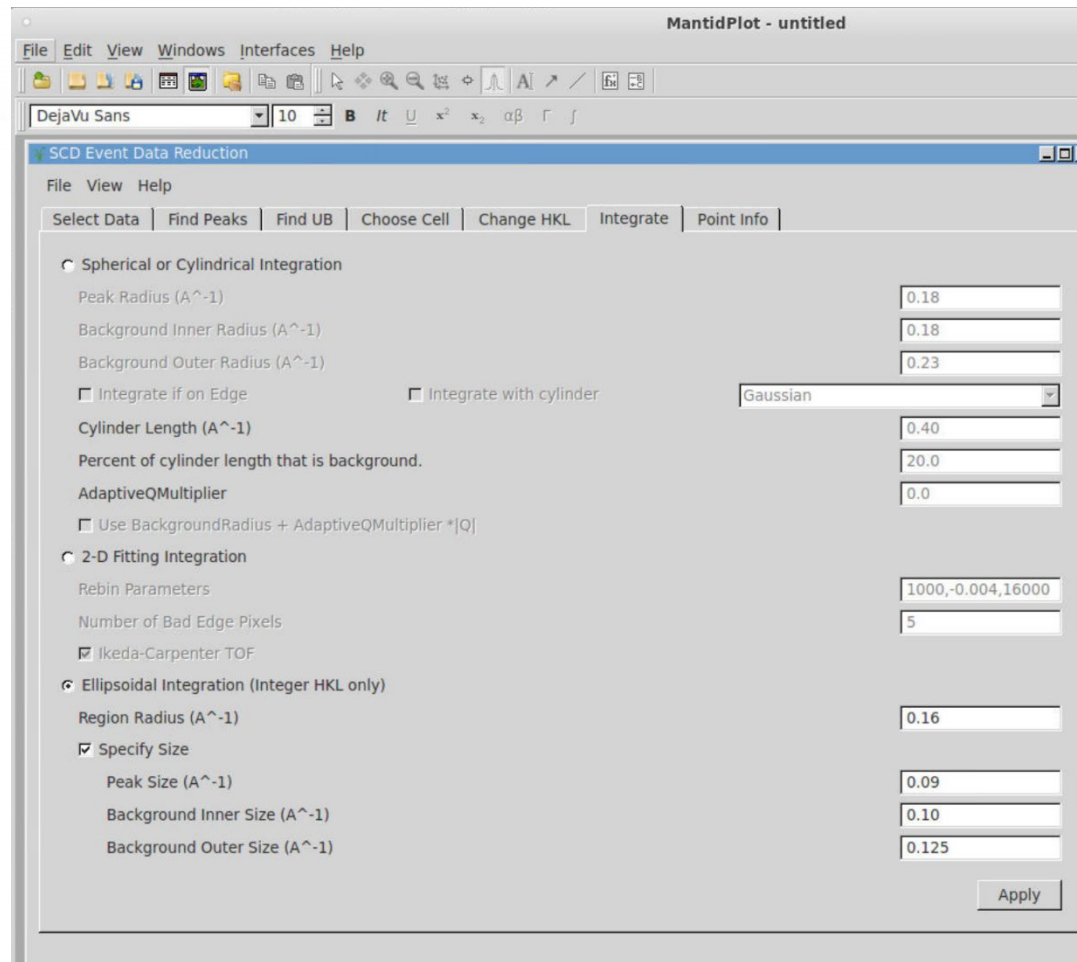


Three-dimensional profile fitting of Bragg peaks in reciprocal space by an Ikeda–Carpenter function with a Bivariate Gaussian

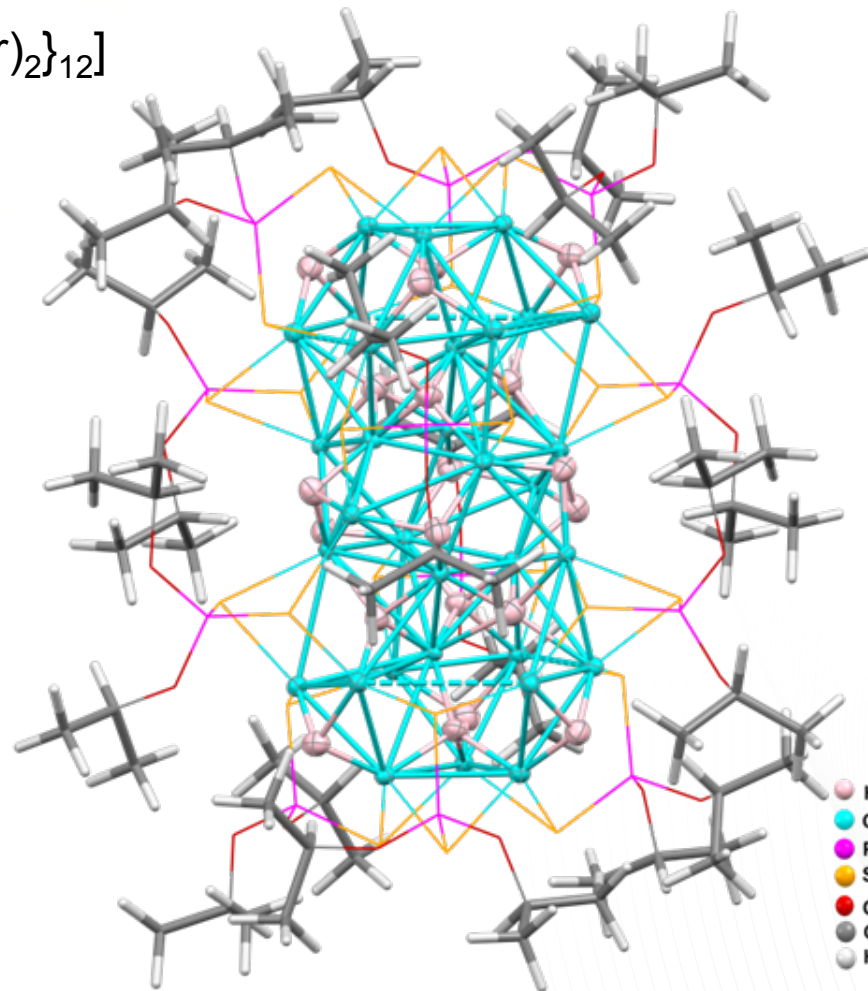
SCD Event Data Reduction Interface in Mantid



SCD Event Data Reduction Interface in Mantid

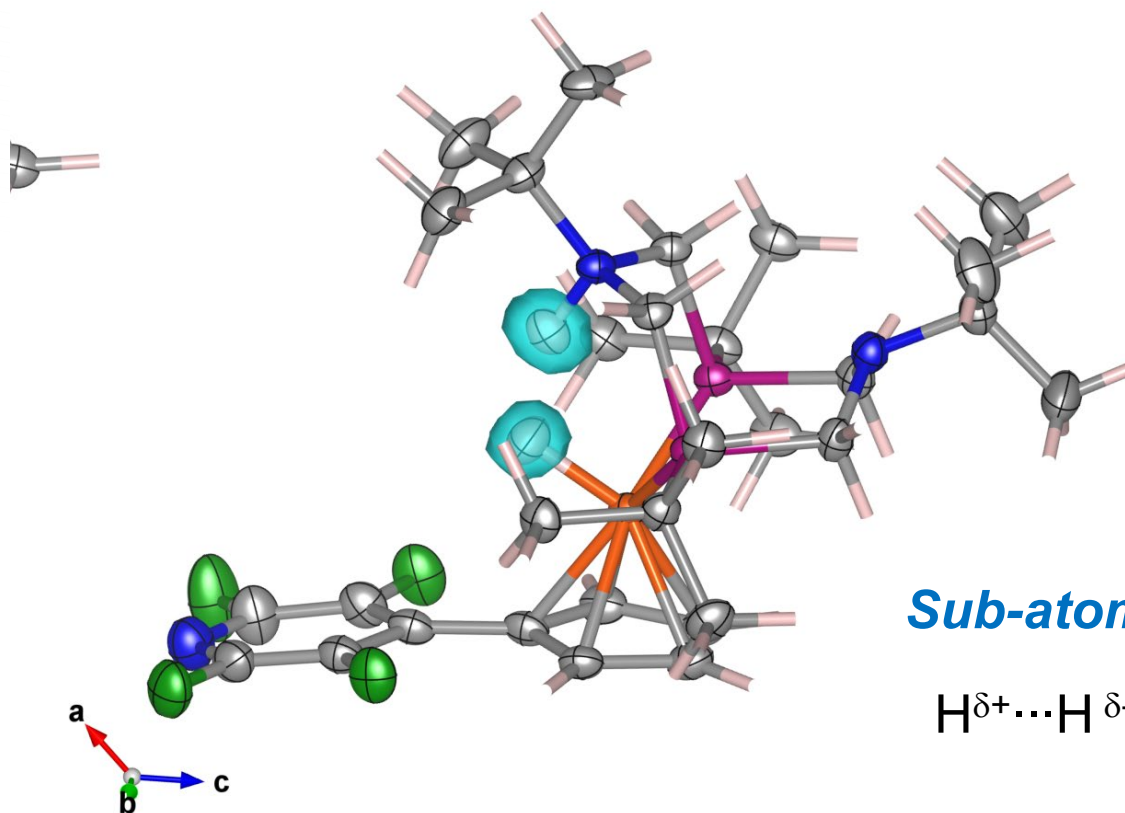


Locate Hydrogen Atoms in a Crystal Structure



A molecular nanocluster by single crystal neutron diffraction

Dihydrogen bond in an electrocatalyst



Sub-atomic resolution

$$\text{H}^{\delta+} \cdots \text{H}^{\delta-} \quad 1.489(10) \text{ \AA}$$

Data reduction in multi-dimensional diffraction space

Incommensurately modulated charged density wave in $K_2V_3O_8$

Shiyun Jin

ORNLGO! Student

Univ. Wisconsin - Madison

Vickie Lynch

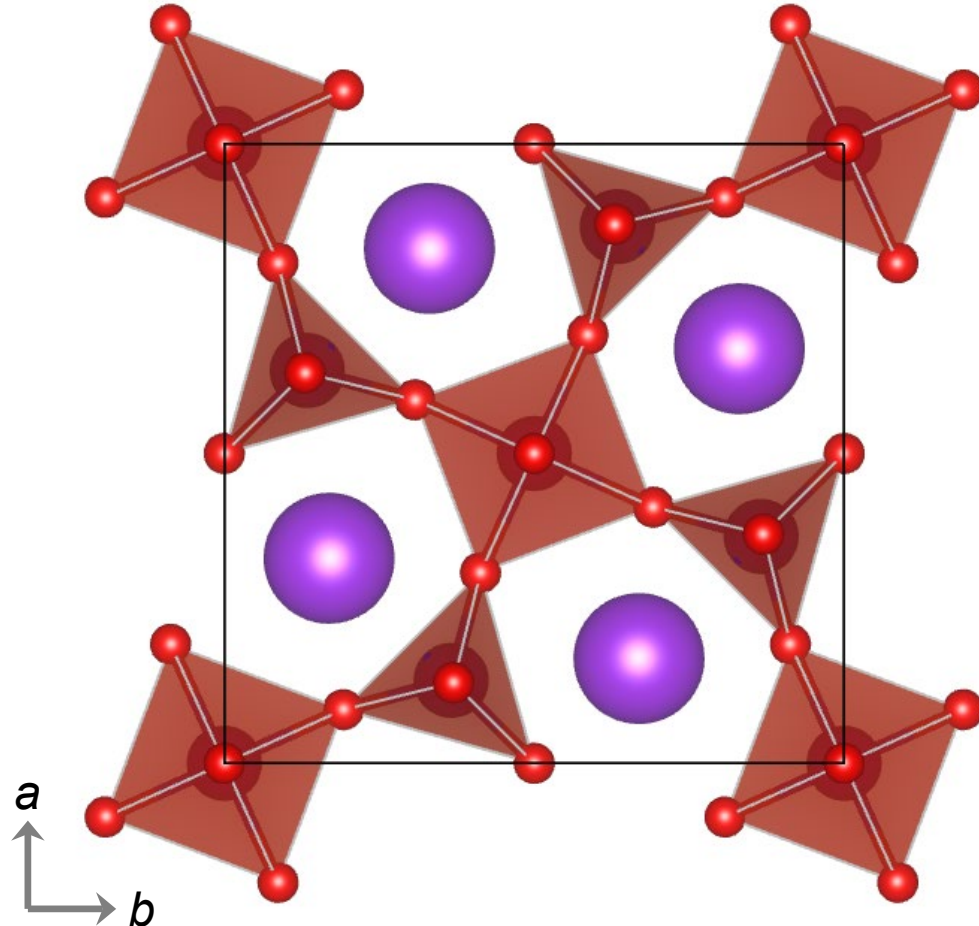
ORNL Software Scientist

A. Banerjee, X.P. Wang, C.M. Hoffmann,
M. Lumsden, B.C. Sales, K.J. Woo, B.C.
Chakoumakos

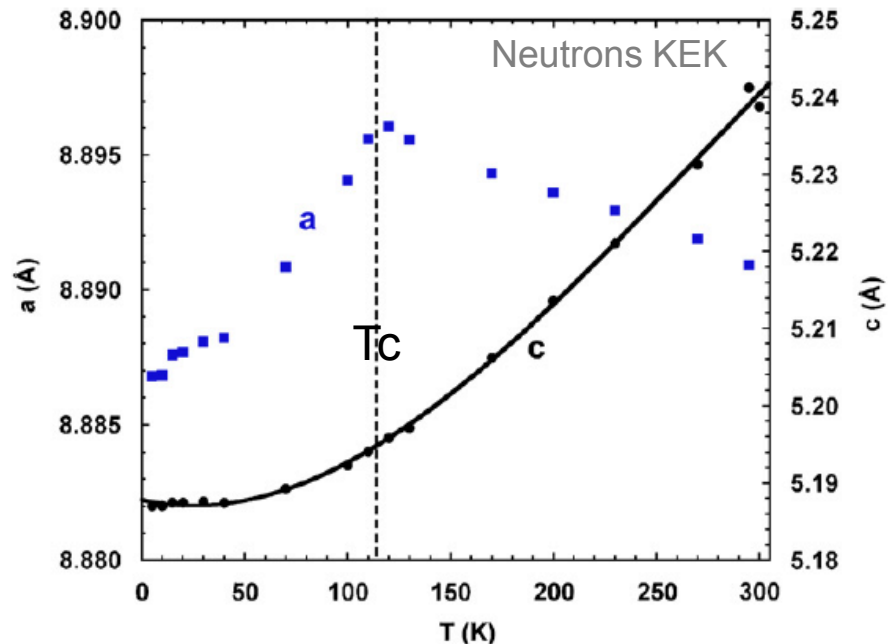
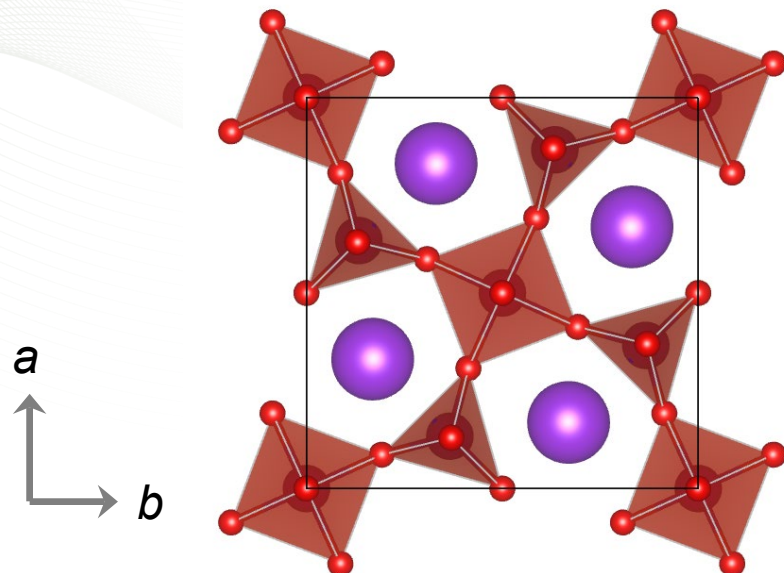


$K_2V_3O_8$ (KVV)

- Fresnoite-type Structure:
 $A_2BC_2O_8$ (ABC)
- A=interlayer Cations
- B=pyramid site
- C=tetrahedral site
- Known materials:
 - $Ba_2TiSi_2O_8$ (BTS)
 - $Ba_2TiGe_2O_8$ (BTG)
 - $Sr_2TiSi_2O_8$ (STS)
 - $Ba_2VSi_2O_8$ (BVS)
 - $Rb_2V_3O_8$ (RVV)
 - $K_2V_3O_8$ (KVV)



Charge ordering in $K_2V_3O_8$



The superlattice modulations happen in the VO layer at :

$$T_c = 110-115 \text{ K}.$$

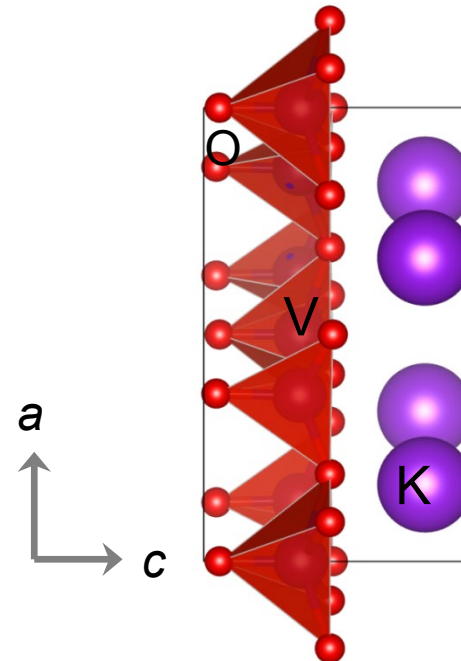
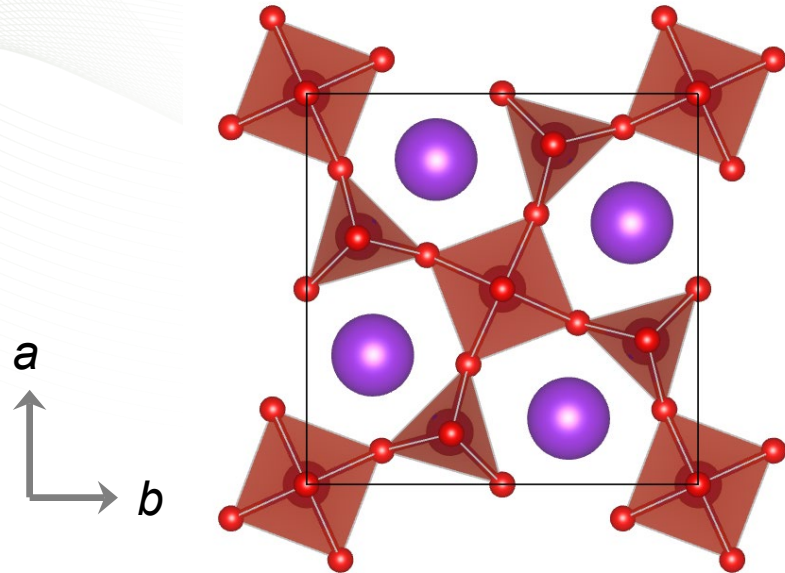
The superlattice modulations are roughly along wave vector:

$$\mathbf{k} = 1/3*[110] * + \frac{1}{2}*[001]*.$$

Possible buckling of basal plane VO layers.

Exact mechanism not known.

Structure of $K_2V_3O_8$

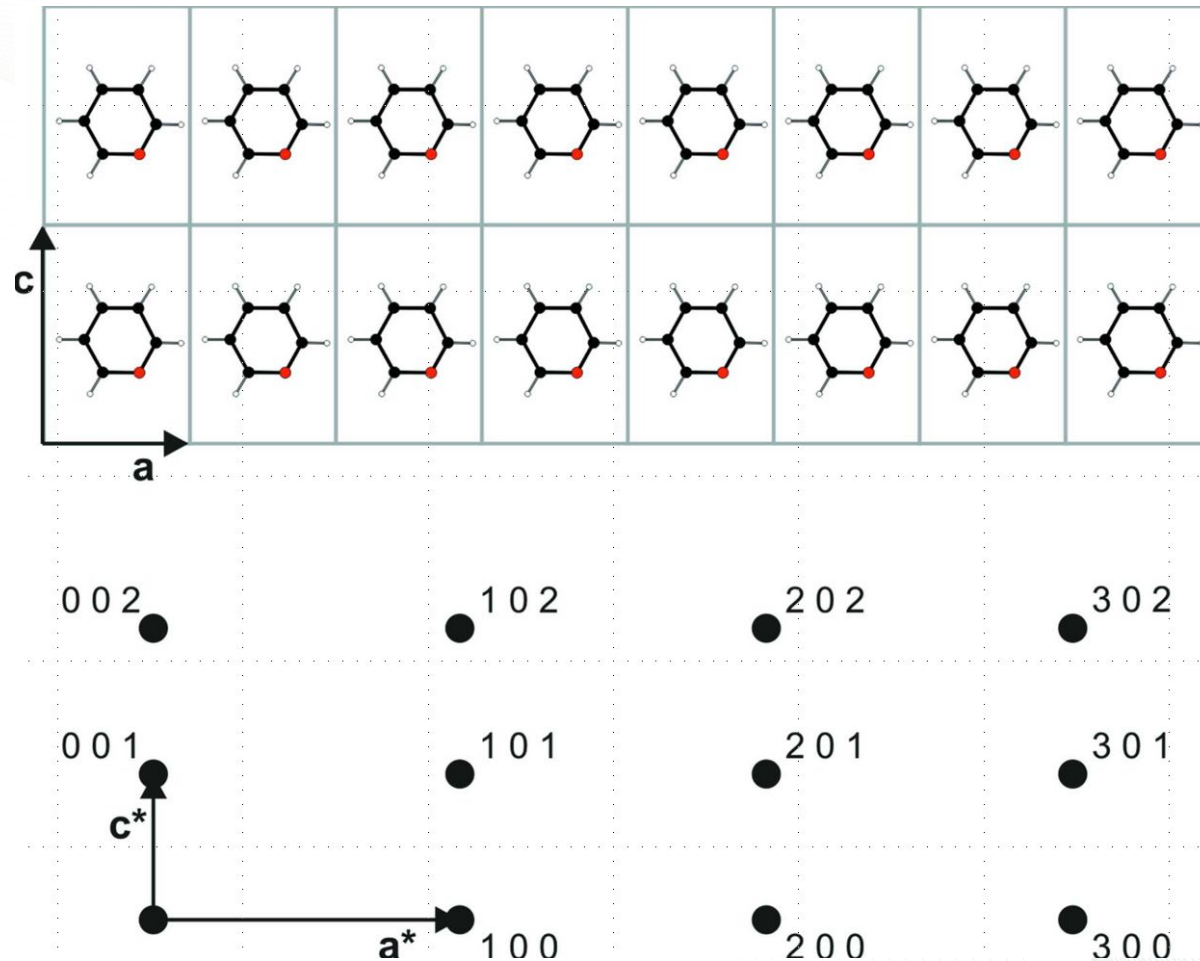


- Alternating K and VO layers.
- Every VO layer has four VO₄ (trigonal) and two VO₅ (tetragonal) pyramids.
- Two Vanadium atom types V⁺⁴ and V⁺⁵

Tetragonal $a = b = 8.8954(1)$ Å, $c = 5.2472(1)$ Å

Superspace description of modulated structures

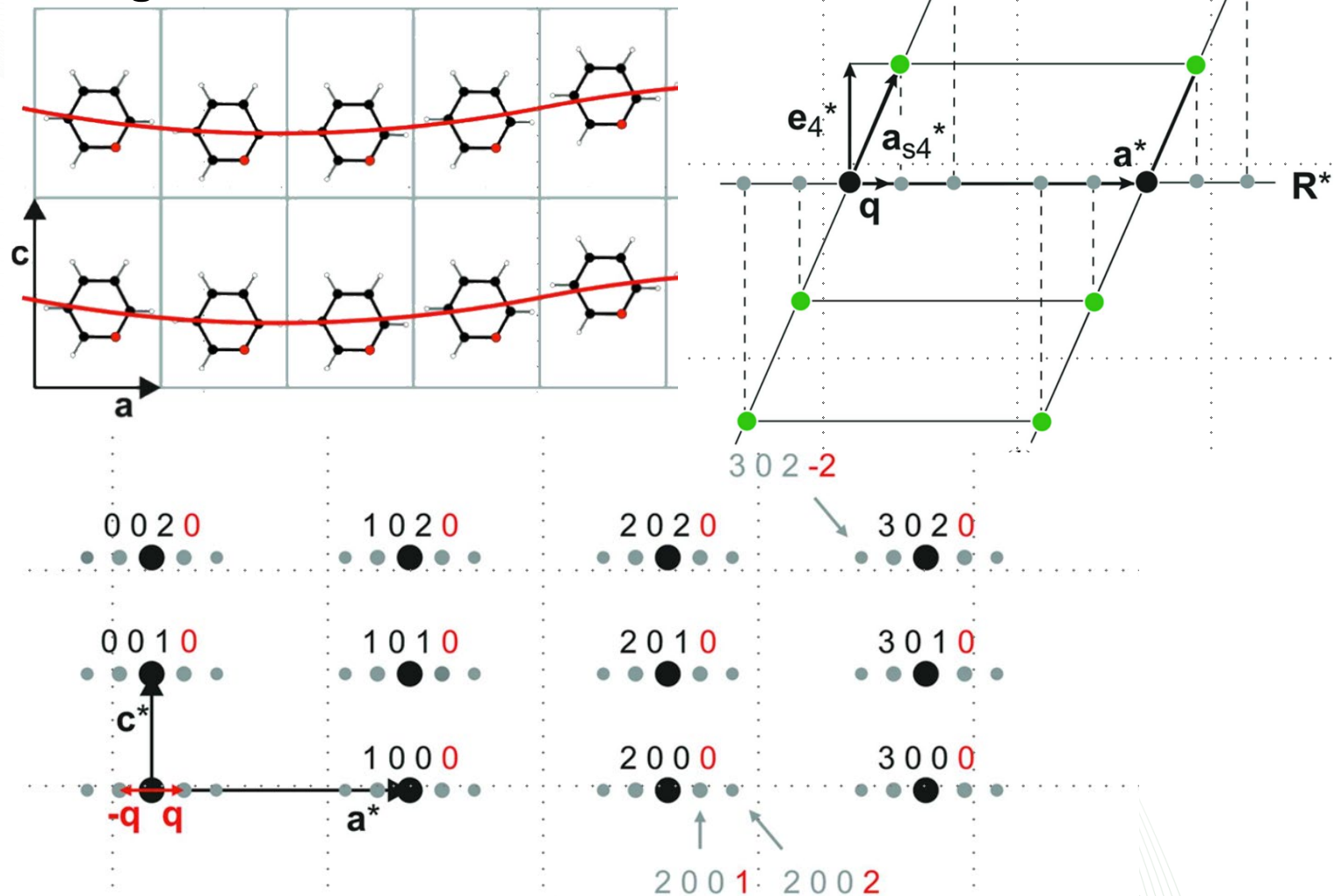
Basic Cell



Wagner & Schönleber, *Acta Cryst. B*, (2009), **65**, 249.

Superspace description of modulated structures

Modulation along the a axis



Wagner & Schönleber, *Acta Cryst. B*, (2009), **65**, 249.

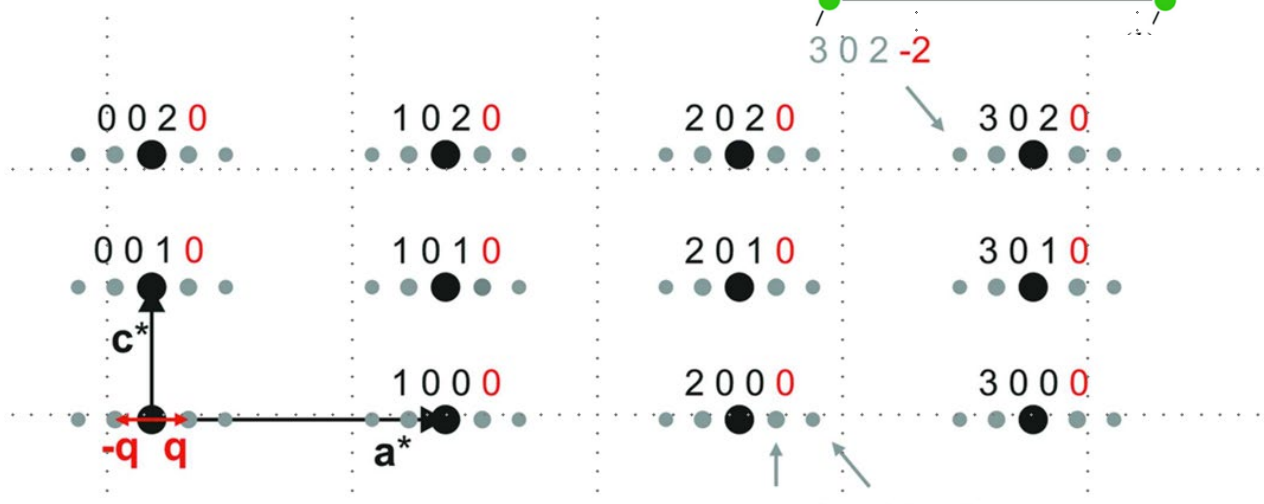
Superspace description of modulated structures

Peak index in $(3 + 1)d$ space

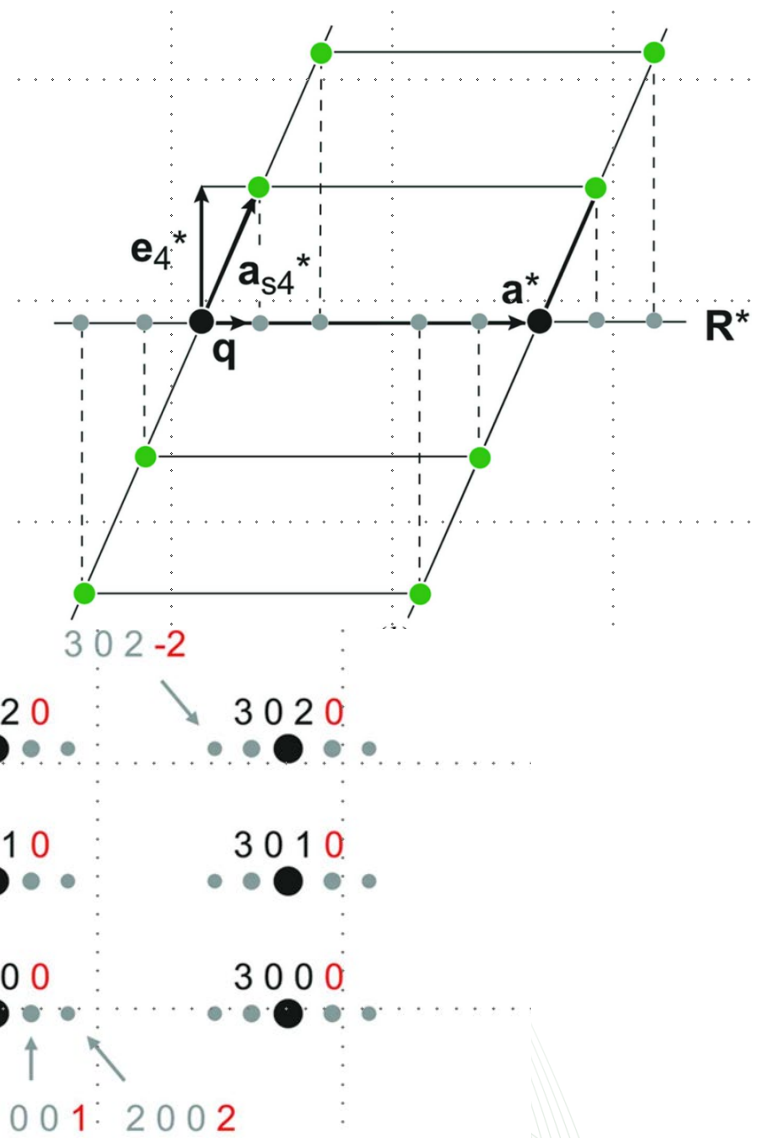
$$\mathbf{q} = 0.125 \cdot \mathbf{a}^* + 0 \cdot \mathbf{b}^* + 0 \cdot \mathbf{c}^*$$

All diffraction spots can be indexed with **4** vectors:

$$\mathbf{H} = h\mathbf{a}^* + k\mathbf{b}^* + l\mathbf{c}^* + m\mathbf{q}$$



Wagner & Schönleber, *Acta Cryst. B*, (2009), **65**, 249.



Types of structural modulation

- The modulation vector \mathbf{q} can be expressed in the reciprocal basis:

$$\mathbf{q} = \alpha \mathbf{a}^* + \beta \mathbf{b}^* + \gamma \mathbf{c}^*$$

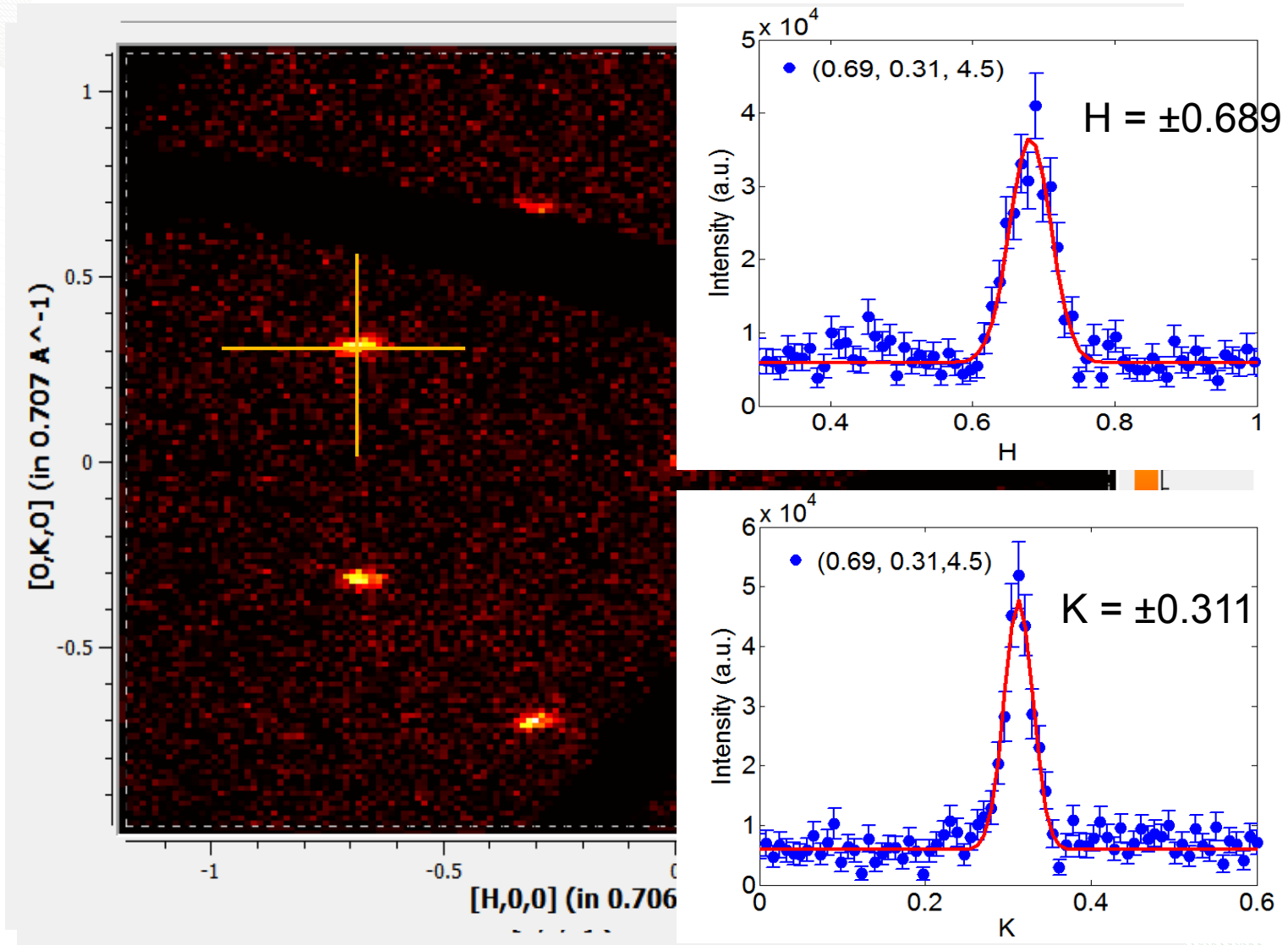
- α, β, γ all rational \rightarrow commensurate structure
- α, β, γ at least one irrational \rightarrow incommensurate structure



Pim de Wolff (1919–1998)

- Incommensurability as an intrinsic crystallographic property was first proposed by de Wolff.
 - Occupational / Displacement
 - Magnetic

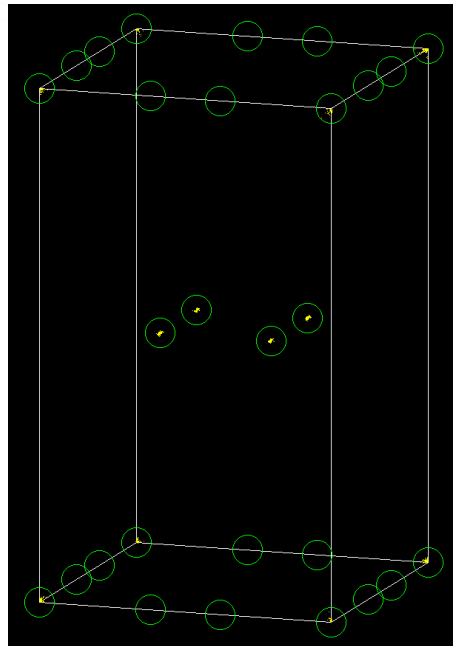
TOPAZ data in $K_2V_3O_8$



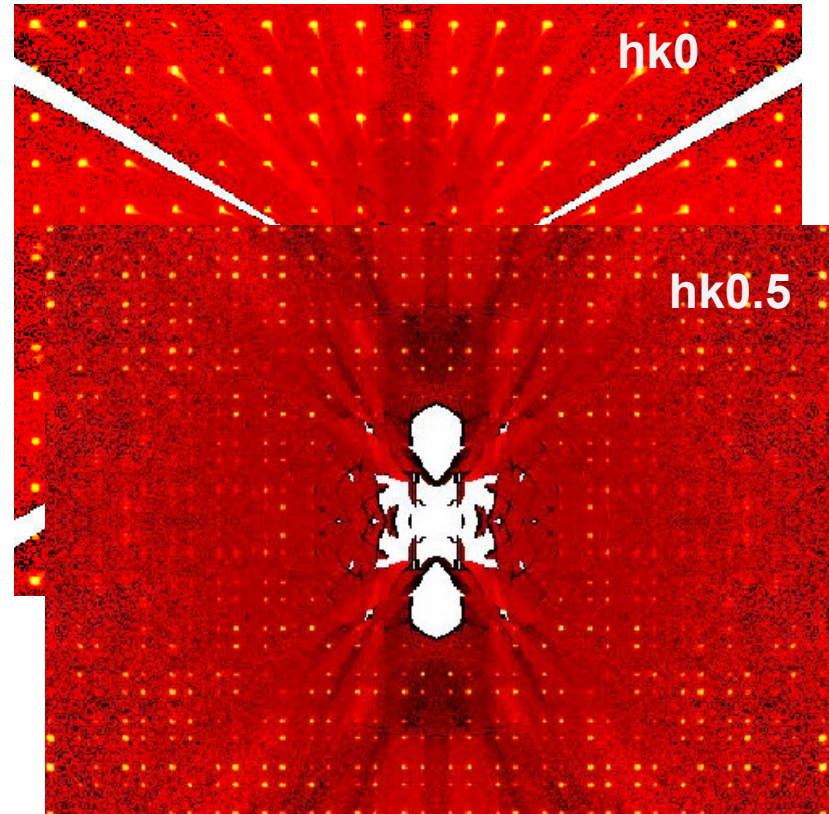
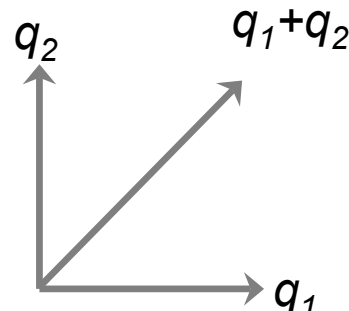
Banerjee

Structure of $K_2V_3O_8$

- Only first order satellites observed
- No cross-terms of satellite observed
- 1d modulation with twinning



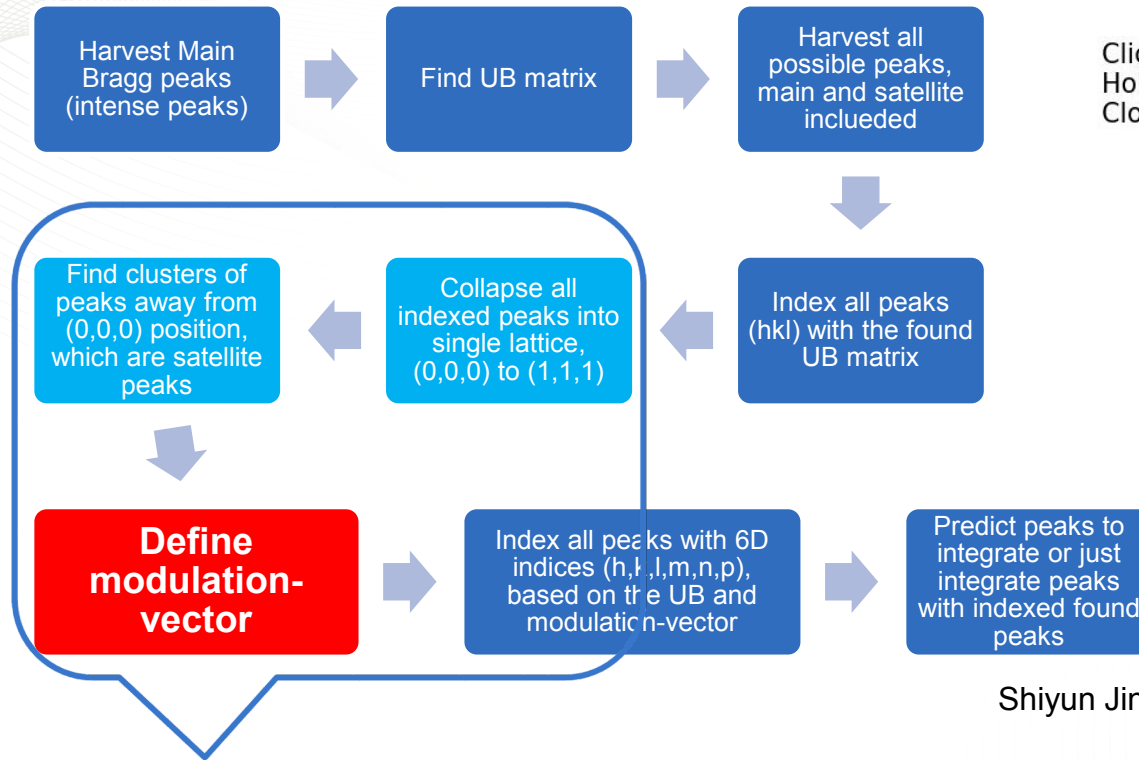
\mathbf{q} vector from JAN2006



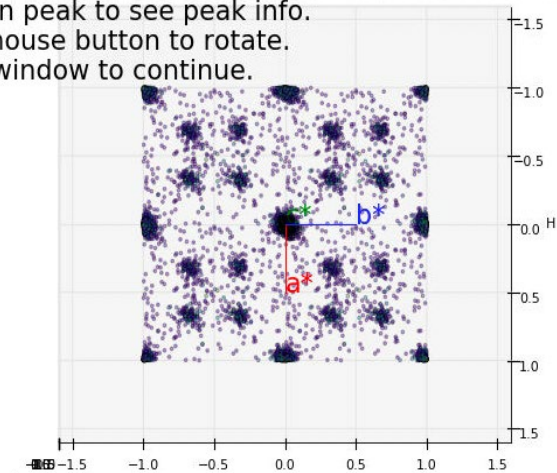
Jin, et al. TOPAZ data

No algorithm available to process satellite peaks in mantid

A User's proposal to reduce satellite peaks



Click on peak to see peak info.
Hold mouse button to rotate.
Close window to continue.



Vickie Lynch

Shiyun Jin

- Almost impossible to automate with an algorithm that works for all situations.
 - Too many possibilities and special cases to consider
- A visualization tool is needed to aid the search for correct Modulation Vector

Update to Mantid

- Added ModUB and ModHKL to Orientedlattice and Unitcell
- Added three IntHKL and IntMNP to peak object
- SavelsawPeaks, LoadlsawPeaks, SavelsawUB, LoadlsawUB** updated accordingly

-0.05056476 -0.05650105 -0.08329089
 0.01945929 0.08565497 -0.07019683
 0.16882414 -0.07853077 -0.04930324
 ModUB:
 0.07499244 -0.03025308 -0.07266121
 0.10634741 0.00508824 -0.02061448
 0.00000000 0.00000000 0.00000000
 8.8763 8.8936 5.1917 90.0497 90.0198 90.1050 409.9318
 0.0016 0.0013 0.0009 0.0129 0.0143 0.0137 0.1193
 Modulation Vector 1: 0.3120 0.3126 0.5016
 Modulation Vector 1 error: 0.0009 0.0010 0.0005
 Modulation Vector 2: -0.3121 0.3124 0.5005
 Modulation Vector 2 error: 0.0013 0.0011 0.0008
 Max Order: 1
 Cross Terms: 0

.mat file for modulated data

Version: 2.0 Facility: SNS Instrument: TOPAZ Date: 2013-05-02T00:00:02 MOD
 6 L1 T0_SHIFT
 7 1800.0398 0.147

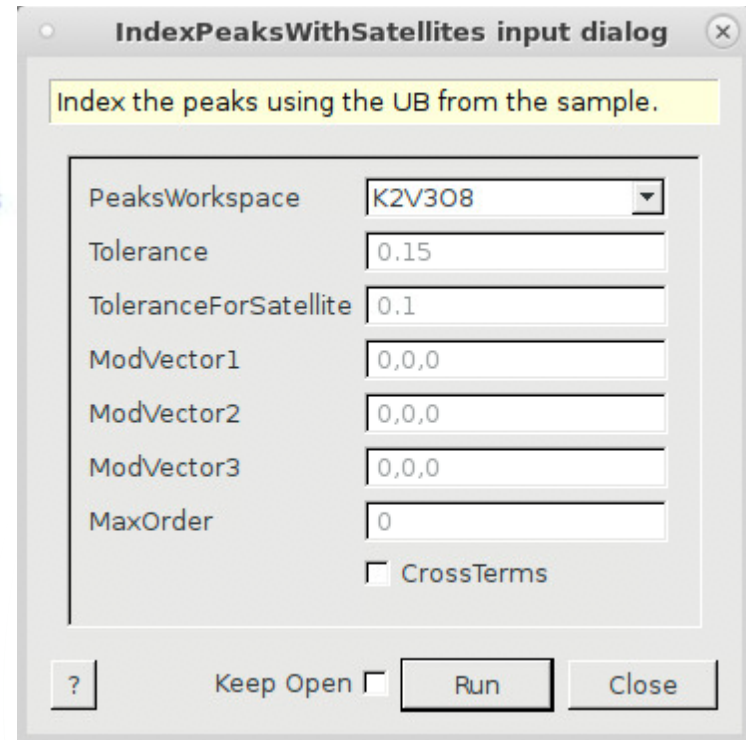
DETNUM	NROWS	NCOLS	WIDTH	HEIGHT	DEPTH	DETD	CenterX	CenterY	CenterZ	BaseX	BaseY	BaseZ	UpX	UpY	UpZ				
5	17	256	256	15.8190	15.8190	0.2000	45.70	-36.8136	-24.2638	-12.0367	-0.13338	0.59900	-0.78956	-0.58205	0.59746	0.55159			
5	18	256	256	15.8190	15.8190	0.2000	45.80	-36.9200	-24.2575	12.0837	-0.57539	0.59806	-0.55790	-0.14114	0.59929	0.78799			
5	22	256	256	15.8190	15.8190	0.2000	43.60	41.9683	-11.8243	0.2580	0.20504	0.67485	0.70890	0.21841	0.67447	-0.70525			
5	26	256	256	15.8190	15.8190	0.2000	42.69	-33.1197	-11.7847	-24.2289	0.26242	0.68209	-0.68256	-0.58640	0.67448	0.44856			
5	27	256	256	15.8190	15.8190	0.2000	42.81	-41.1619	-11.7817	0.0267	-0.18836	0.68004	-0.70856	-0.19801	0.68037	0.70562			
5	28	256	256	15.8190	15.8190	0.2000	42.77	-33.2134	-11.6823	24.2817	-0.58179	0.67421	-0.45492	0.25444	0.68213	0.68554			
5	36	256	256	15.8190	15.8190	0.2000	39.84	-23.2631	0.0522	-32.3407	0.56925	0.70759	-0.41865	-0.57040	0.70662	0.41873			
5	37	256	256	15.8190	15.8190	0.2000	39.74	-37.7856	0.0645	-12.3009	0.21838	0.70737	-0.67226	-0.22016	0.70684	0.67224			
5	38	256	256	15.8190	15.8190	0.2000	39.91	-37.9375	0.1113	12.3835	-0.23401	0.70669	-0.66770	0.23201	0.70752	0.66752			
5	39	256	256	15.8190	15.8190	0.2000	39.92	-23.3841	0.1669	32.3538	-0.57365	0.70556	-0.41607	0.56978	0.70865	0.41614			
5	47	256	256	15.8190	15.8190	0.2000	42.89	-41.1876	11.9584	0.0193	0.19658	0.67912	-0.70721	0.19462	0.67991	0.70700			
5	48	256	256	15.8190	15.8190	0.2000	42.91	-33.2904	11.9812	24.2835	-0.25532	0.67848	-0.68882	0.56618	0.68242	0.46232			
5	58	256	256	15.8190	15.8190	0.2000	45.92	-36.9495	24.4692	12.0435	0.14027	0.59983	-0.78774	0.57174	0.60048	0.55905			
0	NRUN	DETNUM	CHI	PHI	OMEGA		MONCNT												
1	8091	17	135.00	-153.72	169.64		39536066												
2	SEQN	H	K	L	M	N	P	COL	ROW	CHAN	L2	2_THETA	AZ	WL	D	IPK	INTI	SIGI	RFLG
9	0	-1	17	-7	0	0	0	37.00	221.00	3216	46.581	1.88040	-2.75424	0.689054	0.4266	26	13.75	6.70	310
9	1	-1	15	-6	0	0	0	19.00	234.00	3640	46.547	1.85096	-2.75308	0.779783	0.4880	51	50.38	9.31	310
9	2	-1	12	-5	0	0	0	218.00	203.00	4526	46.295	1.87527	-2.71868	0.969863	0.6015	158	313.19	18.77	310
9	3	-1	10	-4	0	0	0	186.00	219.00	5403	46.220	1.82833	-2.70943	1.157807	0.7309	1596	3214.97	58.75	310

.peaks file for modulated data

Update to Mantid

```
Lattice Parameters: 8.899332 8.880559 5.193367 90.133085 89.989240 89.995700 410.436063  
Parameter Errors : 0.000062 0.000063 0.000029 0.000516 0.000516 0.000568 0.004690  
Modulation Dimension is: 2  
Modulation Vector 1: [0.309944,0.310118,0.499995]  
Modulation Vector 1 error: [0.001678,0.001914,0.001099]  
Modulation Vector 2: [-0.309953,0.310125,0.500008]  
Modulation Vector 2 error: [0.001669,0.001898,0.001101]  
FindUBUsingIndexedPeaks successful, Duration 14.93 seconds
```

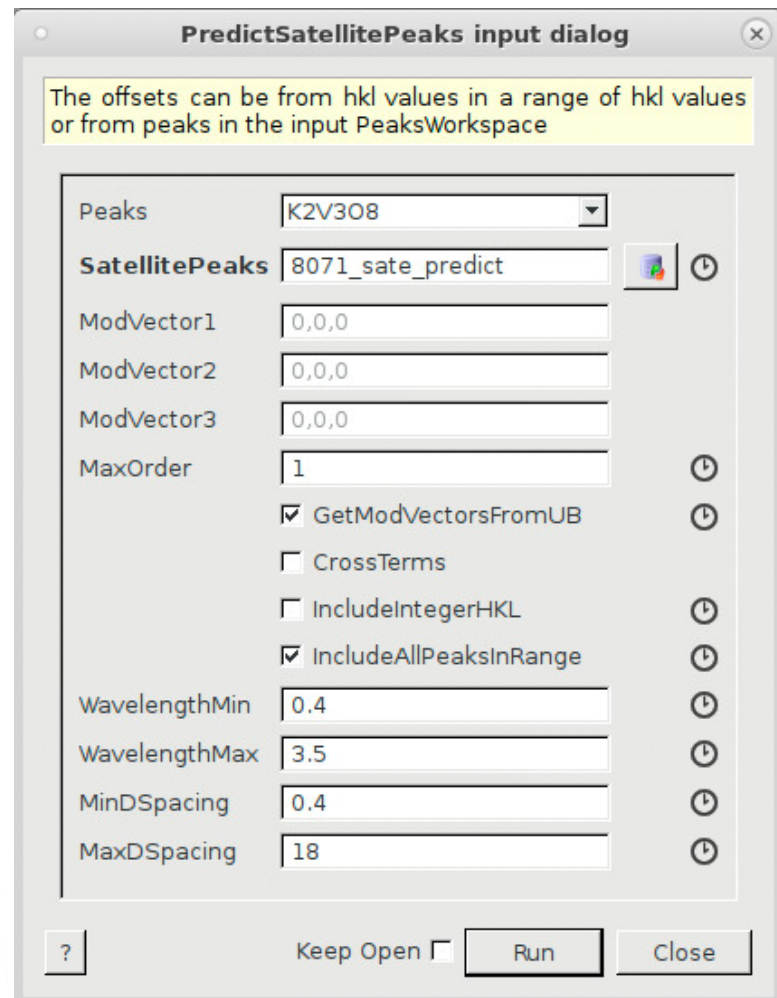
- **IndexPeaksWithSatellites**
- Allow user to put in estimated modulation-vector to index satellite peaks (and main peaks)
- **FindUBUsingIndexedPeaks**
- can find optimized UB and ModUB with indexed peaks including satellite peaks.
- IndexPeaks can index satellite peaks as well if required information is stored in UB and ModUB



```
ALL Runs: indexed 194274 Peaks out of 194308 with tolerance of 0.1  
Out of 194274 Indexed Peaks 23099 are Main Bragg Peaks, and 171175 are satellite peaks  
Average error in h,k,l for indexed peaks = 0.00411508  
Average error in h,k,l for indexed main peaks = 0.00829558  
Average error in h,k,l for indexed satellite peaks = 0.00355095
```

Update to Mantid

- PredictSatellitePeaks
- Predict all the peaks within range that is allowed by the UB and modulation vector.
- Modulation vector can be read from peakworkspace or input by user
- Predicted peaks list is already properly indexed with 6d indices (h,k,l,m,n,p)
- See details in Mantid Concept for
 - [Modulated Structure](#)



Time filtering of event based neutron scattering data

Real-Time observation of organic cations induced phase transition in hybrid perovskites

Bing Yang

Postdoc, ORNL Center for Nanophase Materials
Currently Professor at Hunan University, China

Ming W., Du M., Keum J.K., Puretzky A.,
Rouleau C.M., Huang J., Geohegan D.B.,
Wang X.P., Xiao K.

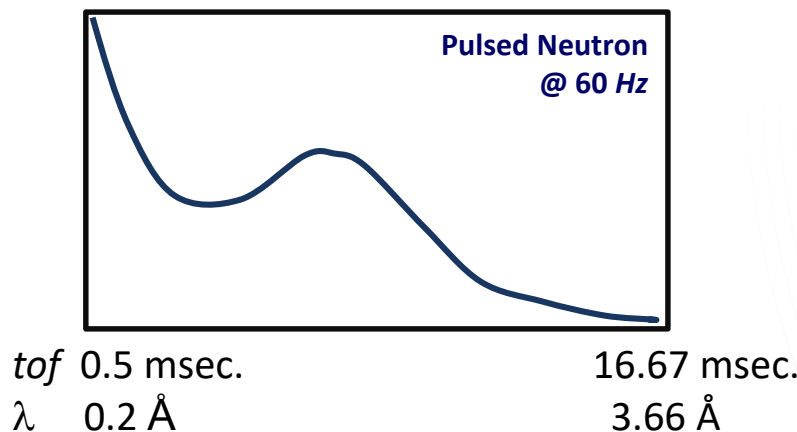


Neutron Time-of-Flight, TOF

- **Neutron Time of Flight:** Event based neutron detection technique
 - de Broglie equation relates neutron wavelength to its momentum:

$$\lambda = \frac{h}{mv} = \frac{h}{m} \frac{t}{L} = \frac{h}{m} \frac{t}{(L_1 + l_2)}$$

- By recording the time of a neutron arrives over a fix path length (aka **time of flight**), its velocity, and consequently its wavelength can be measured.

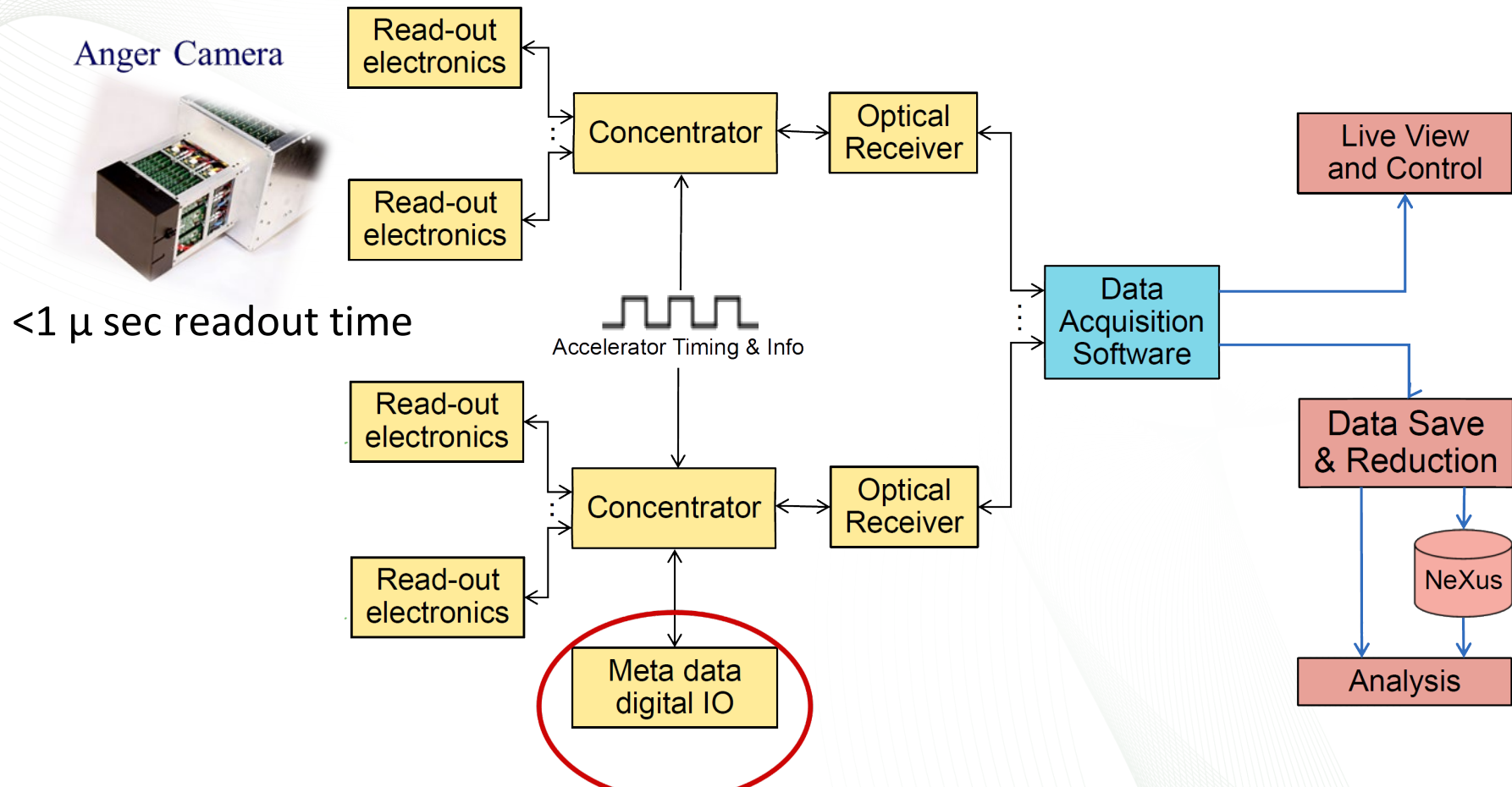


Anger Camera



<1 μ sec readout time

Data Acquisition System at SNS Instruments

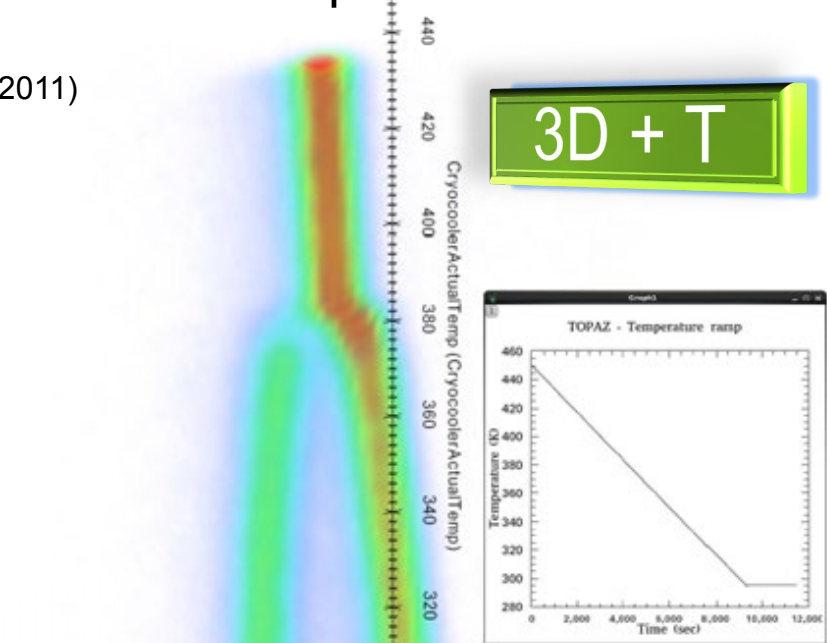


SNS Real Time Data Link (RTDL), a 10 MHz, bi-phase mark encoded serial link.
Signals have **100 nanosec.** resolution.

Time filtering of event data

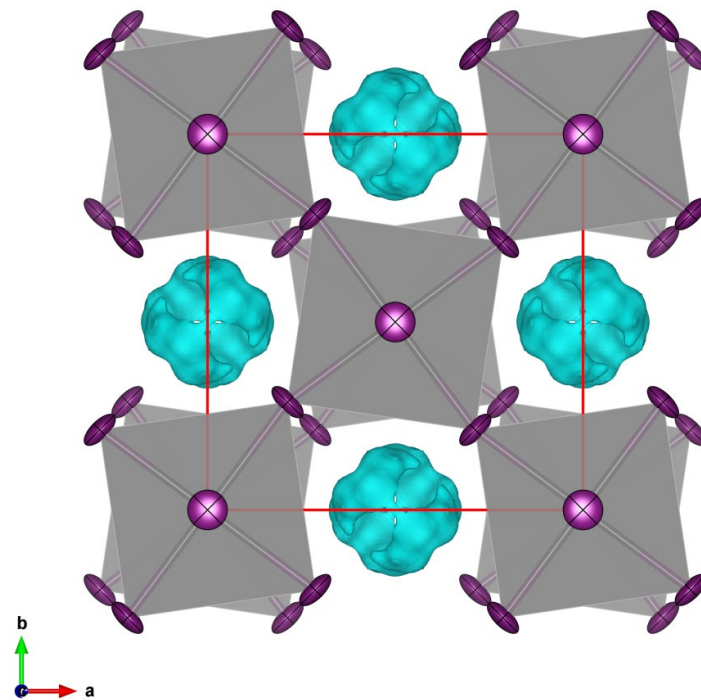
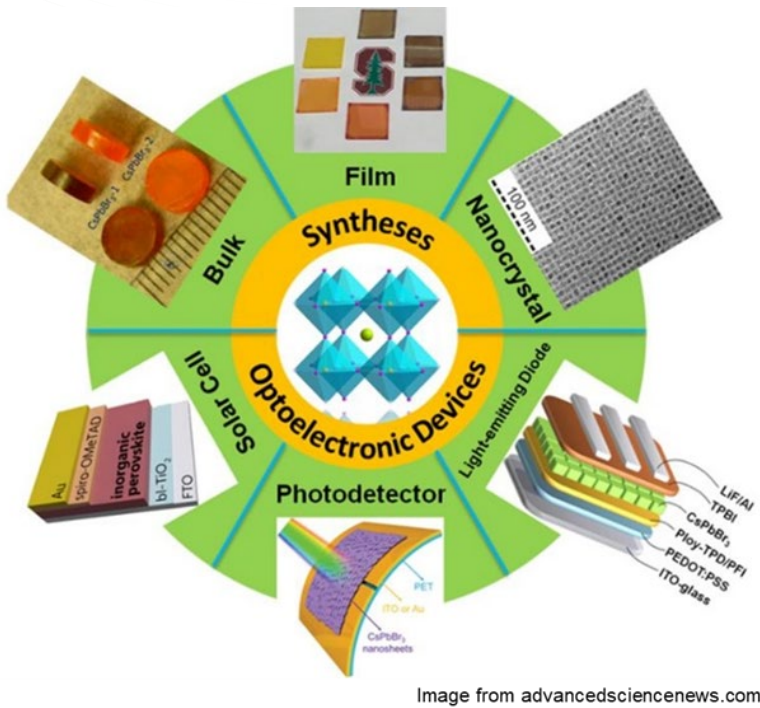
Variable temperature study

- Place preselected Bragg peak on selected detector position
 - CrystalPlan
Zikovsky et al. J. Appl. Cryst., **44**, 418 (2011)
- Measure while heating / cooling
 - Stationary single crystal
 - Neutron recorded in event mode
 - Detector pixel position (x,y)
 - Neutron time of flight (λ)
 - Sample temperature (T, K)
 - Link to event data with a time stamp
- Data saved as event nexus file



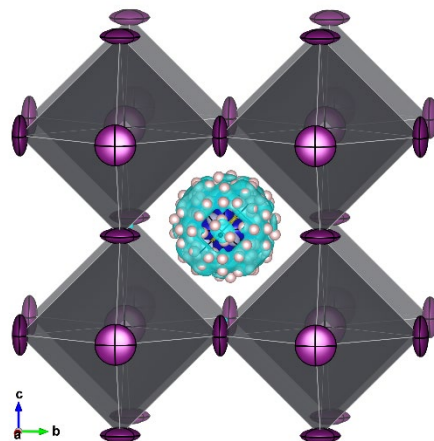
Hydrogen bonding in hybrid perovskites

- High power conversion efficiencies (> 22%) for solar cell applications
 - Heavy elements with very high X-ray absorption $\mu = 526.82 \text{ cm}^{-1}$
 - **Transparent to neutrons** $\mu = 0.654 + 0.508\lambda \text{ cm}^{-1}$
- Effect of H-bonding on structural phase transitions, $\text{CH}_3\text{NH}_3\text{PbI}_3$

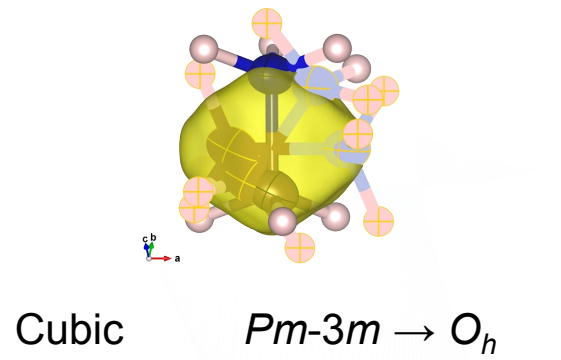
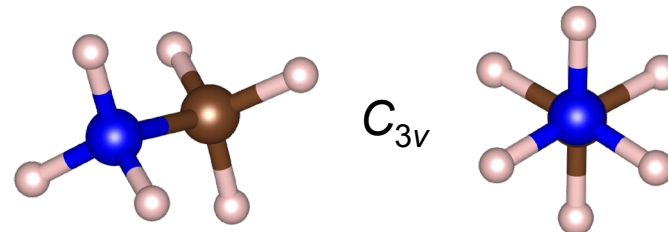


Hybrid Organic Inorganic Perovskite

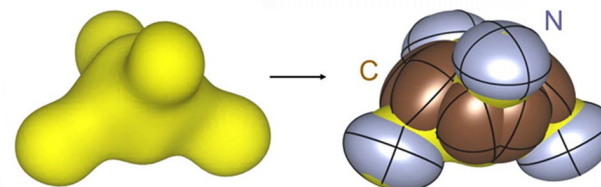
- MAPbX_3
 - MA C_{3v} point group symmetry
 - Crystal site symmetry is higher than that of the molecule symmetry



Disordered MA

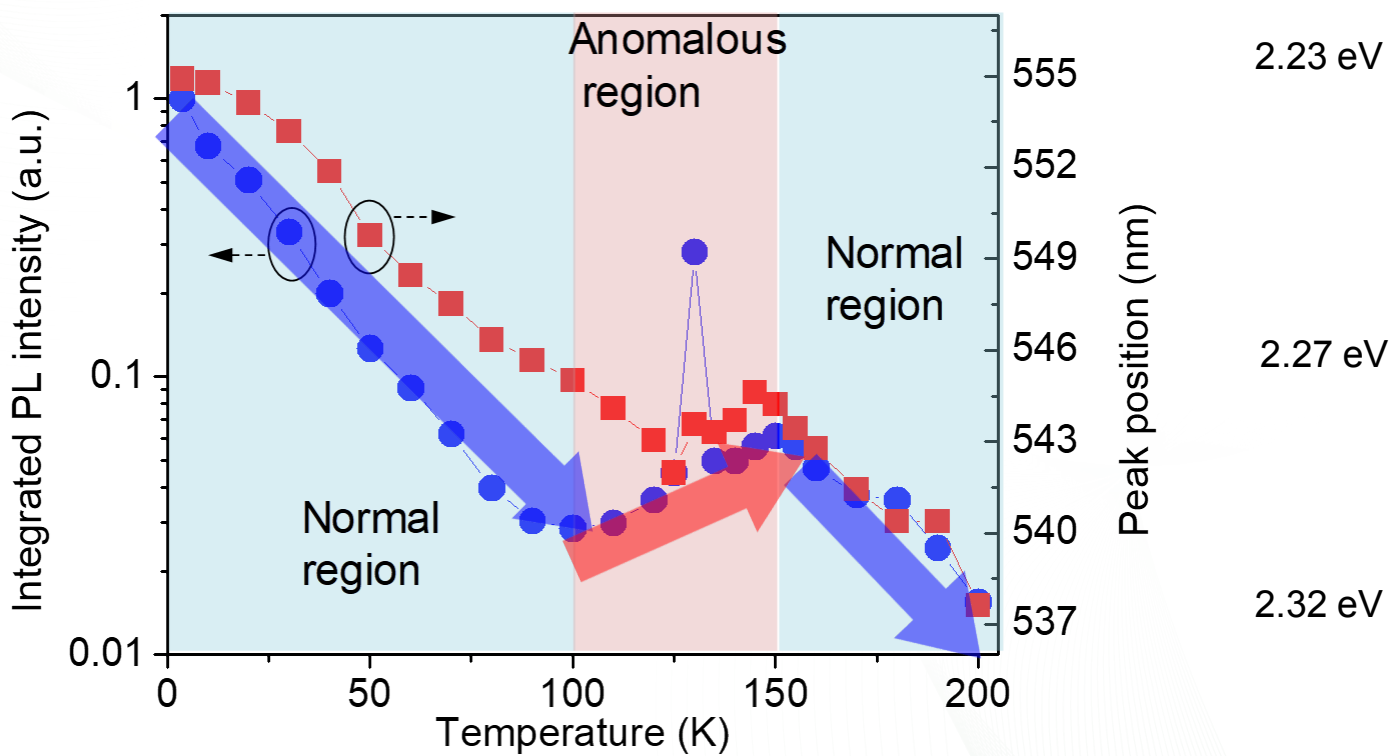


Cubic $Pm-3m \rightarrow O_h$



Tetragonal $I4/mcm \rightarrow D_{2d}$

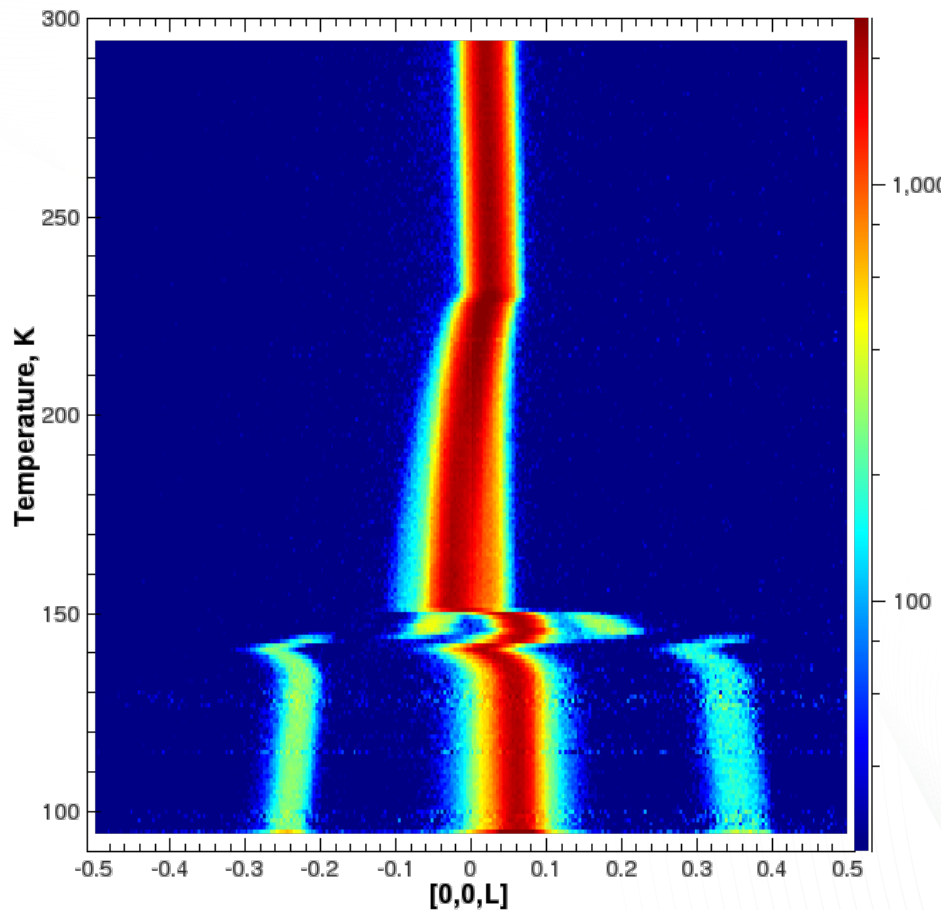
Optoelectronic property of MAPbBr_3



Integrated PL peak intensity (blue circles) and PL peak positions (red squares), where *light pink region* indicates anomalous region

MAPbBr₃ peak profile

MAPbBr₃ (Heating rate 1 K min⁻¹)



Cubic

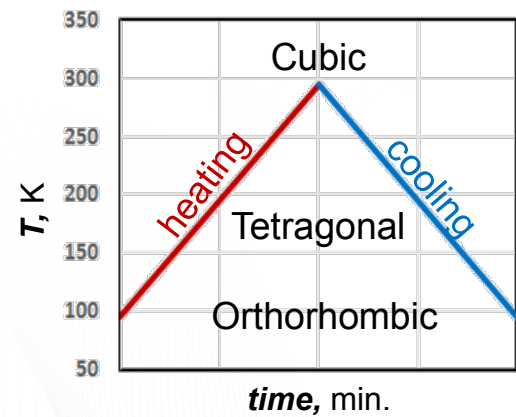
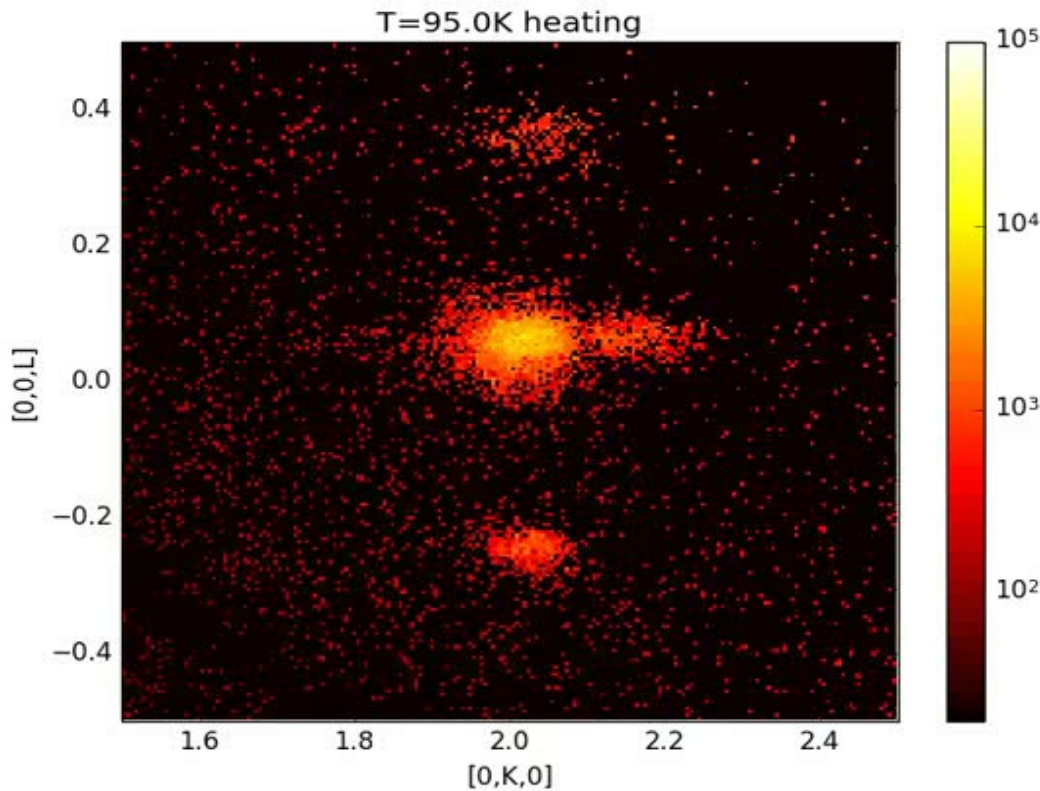
Tetragonal

Orthorhombic

Temperature dependence of the $(2\ 0\ 0)_C$ peak

Peak splitting of MAPbBr_3

Evolution of the o- MAPbBr_3 $(202)_\text{O}$ peak upon continuous heating from 95 K to 295 K and cooling from 295 K to 95 K at the rate of 1 K/min.

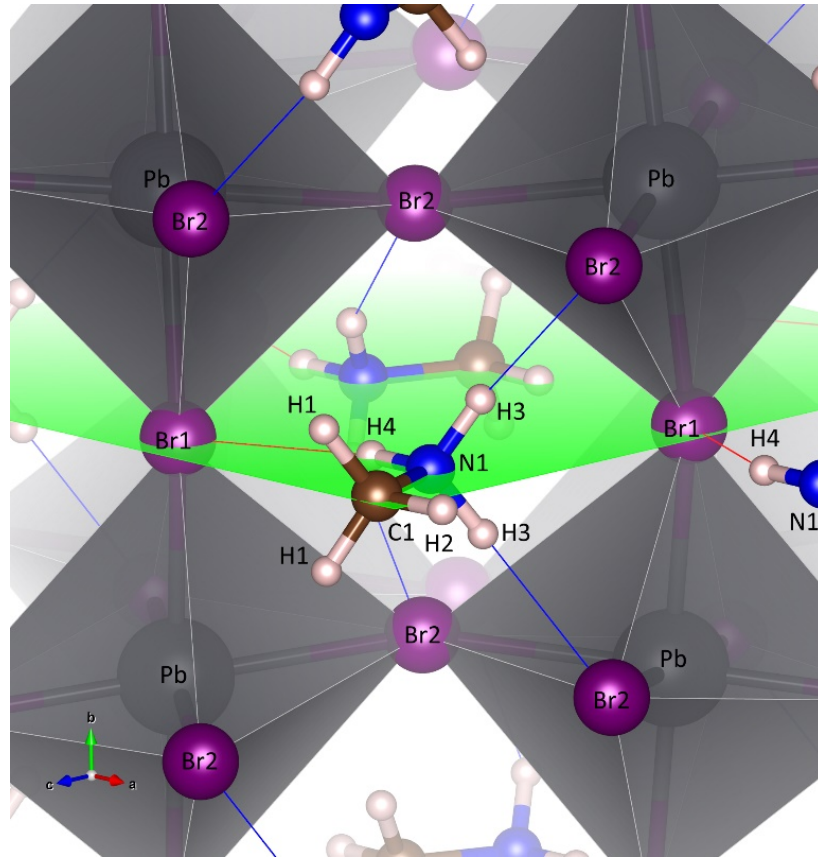


Ramping rate 1K per min.

$$(202)_\text{O} / (220)_\text{T} / (200)_\text{C}$$

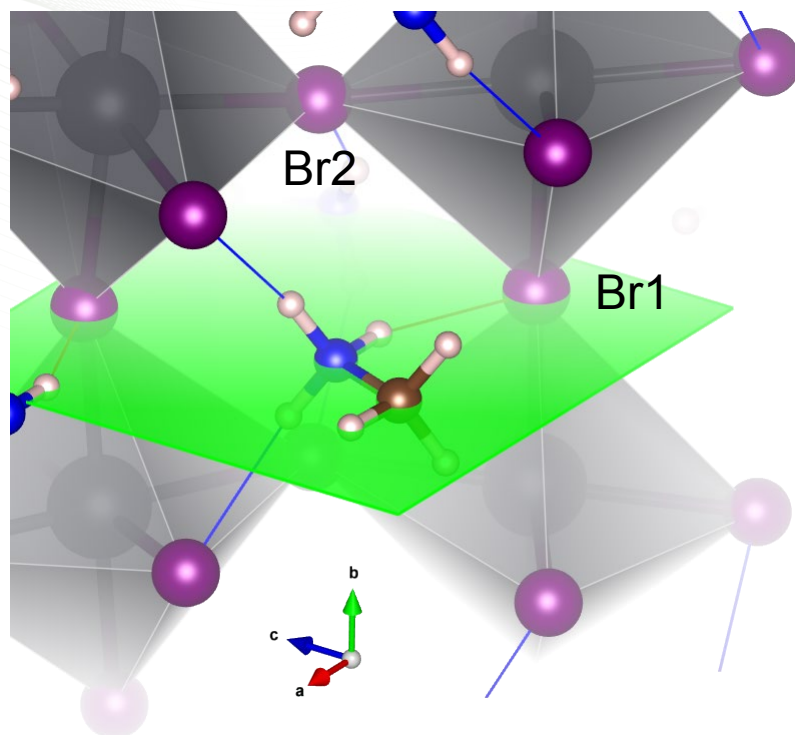
Hydrogen bonding interactions in MAPbBr_3

Orthorhombic *Pnma* structure



Neutron structure of MAPbBr_3 at 95 K. The **blue** and **red** lines represent the trifurcated hydrogen bonds between hydrogen atoms on the $-\text{NH}_3^+$ terminal of the MA cation and the bromides on the PbBr_6 octahedra.

Hydrogen bonding and octahedral tilting

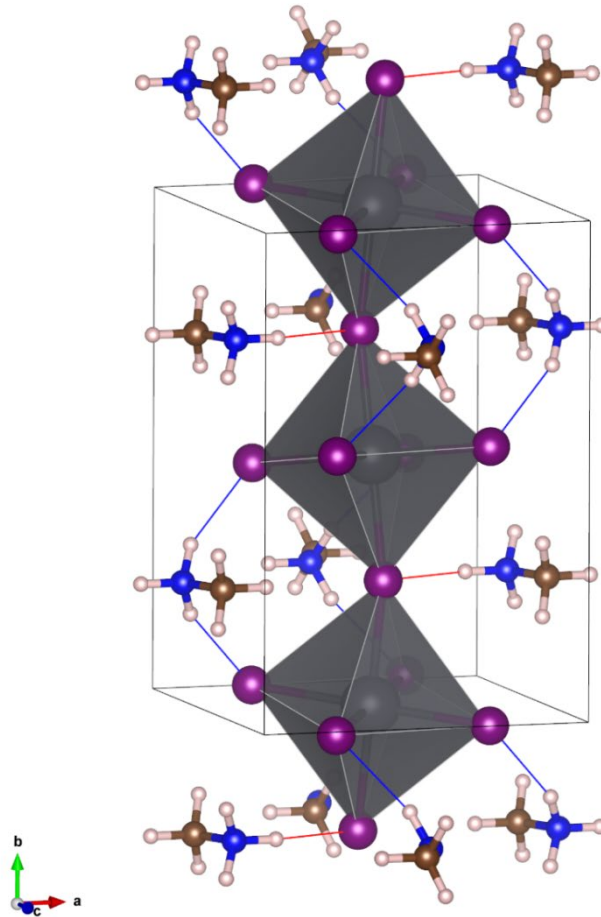


Apical along *b* in SG *Pnma*

$\phi_{(\text{Pb-Br1-Pb})}$ 168.80(19) $^\circ$ Glazer *b*⁺

Equatorial along {1 0 1}

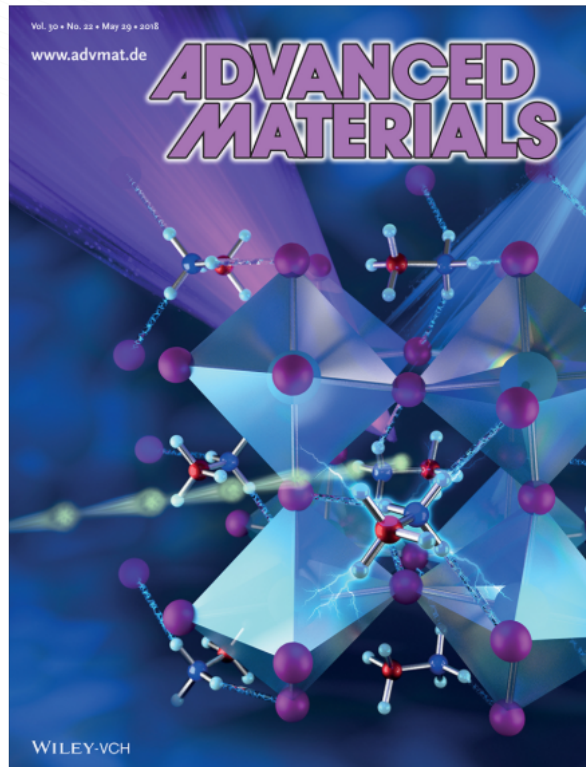
$\phi_{(\text{PB-BR2-PB})}$ 156.80(18) $^\circ$ Glazer *a*⁻



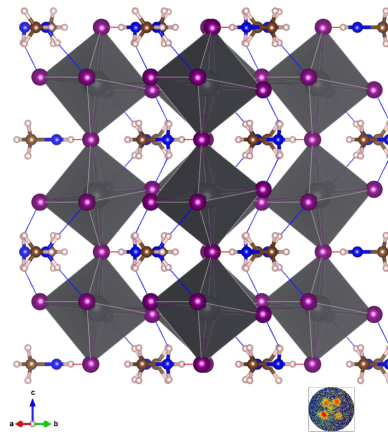
Organohalide Perovskites: Real-Time Observation of Order-Disorder Transformation of Organic Cations Induced Phase Transition and Anomalous Photoluminescence in Hybrid Perovskites (Adv. Mater. 22/2018)

Bin Yang, Wenmei Ming, Mao-Hua Du, Jong K. Keum, Alexander A. Puretzky, Christopher M. Rouleau, Jinsong Huang, David B. Geohegan, Xiaoping Wang, Kai Xiao

1870158 | First Published: 24 May 2018



In article number 1705801, Xiaoping Wang, Kai Xiao, and co-workers describe real-time, in situ temperature-dependent neutron-diffraction/photoluminescence measurements that reveal an order-to-disorder transformation of the organic cation MA^+ with increasing temperature, at the molecular level, in a hybrid organic-inorganic perovskite, MAPbBr_3 , which leads to an anomalous photoluminescence enhancement due to reduced nonradiative recombination.

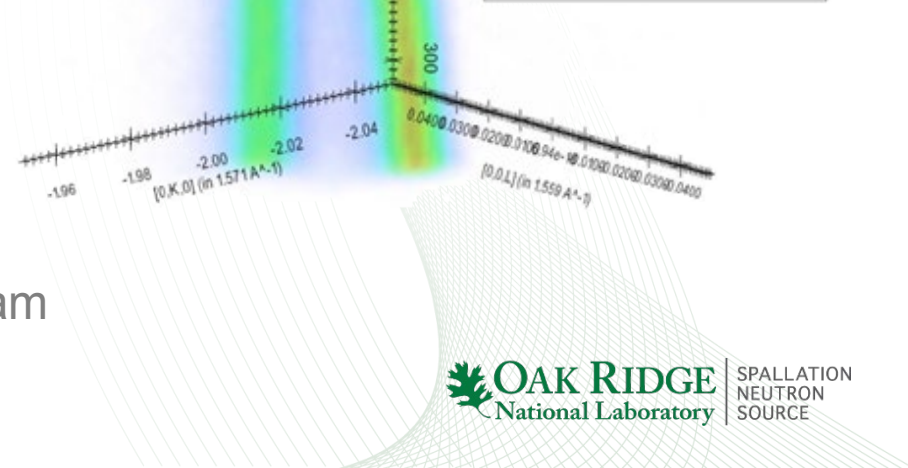
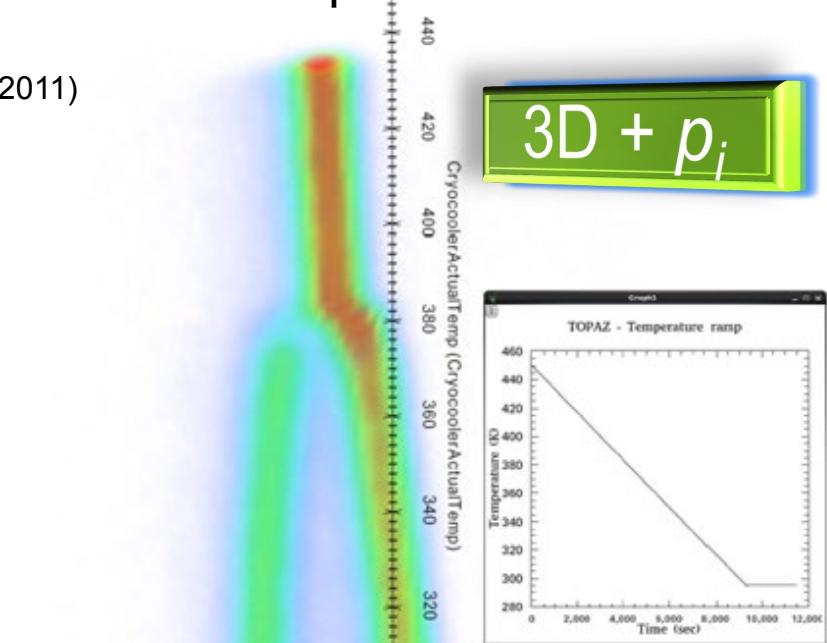


Time filtering of event data

Variable temperature study

- Place preselected Bragg peak on selected detector position
 - CrystalPlan
Zikovsky et al. J. Appl. Cryst., **44**, 418 (2011)
- Measure while heating / cooling
 - Stationary single crystal
 - Neutron recorded in event mode
 - Detector pixel position (x,y)
 - Neutron time of flight (λ)
 - Sample temperature (T, K)
 - Link to event data with a time stamp
- Data saved as event nexus file
- 3D diffraction data + external stimuli
 p_i with $i = 1 \dots n$

Static and Pulsed E-field: In user program



Time filtering of event based neutron scattering data

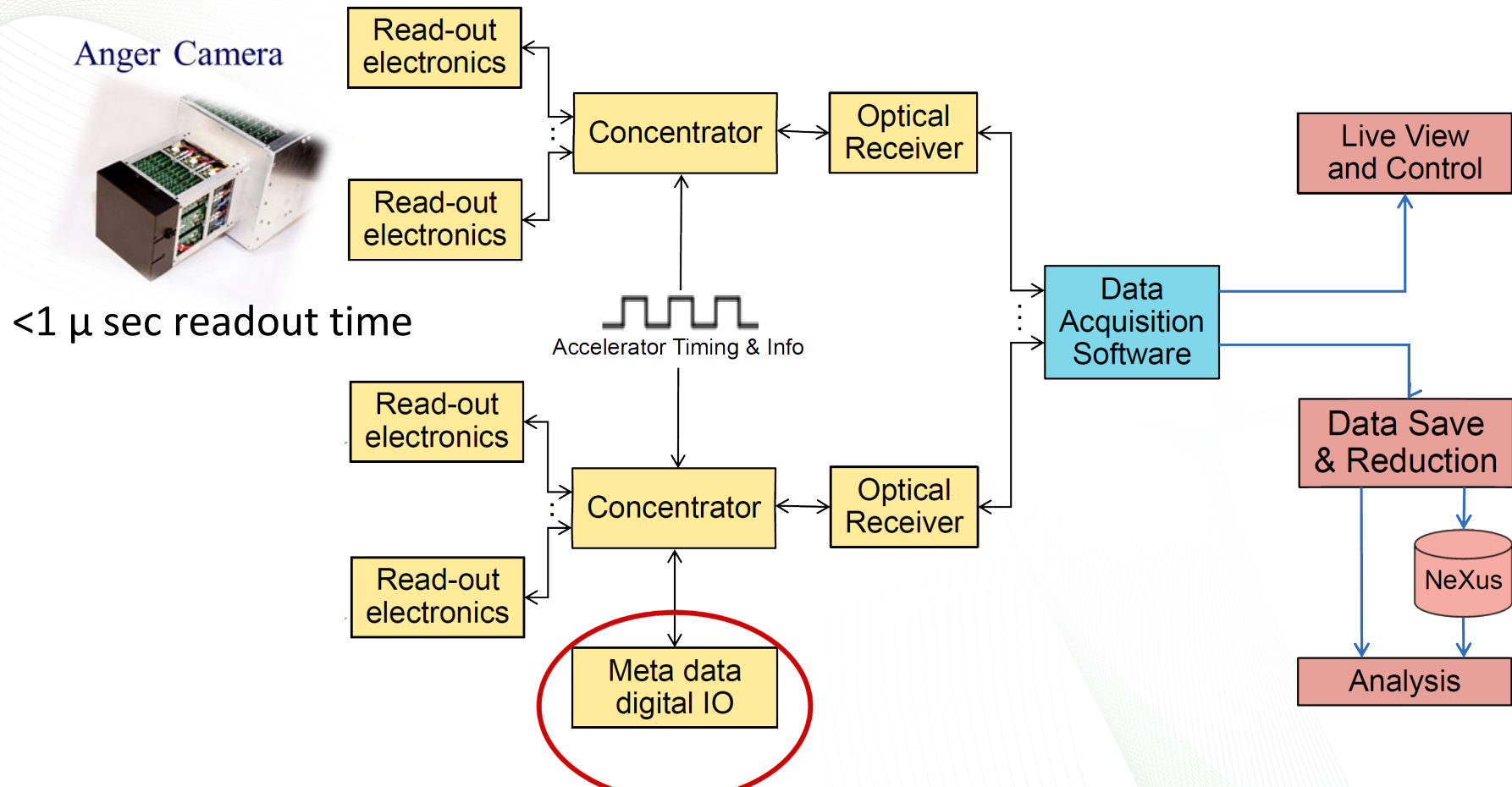
Dynamic structural response of materials in pulsed electric field

Christopher M. Fancher

Postdoc, ORNL Neutron Scattering Division

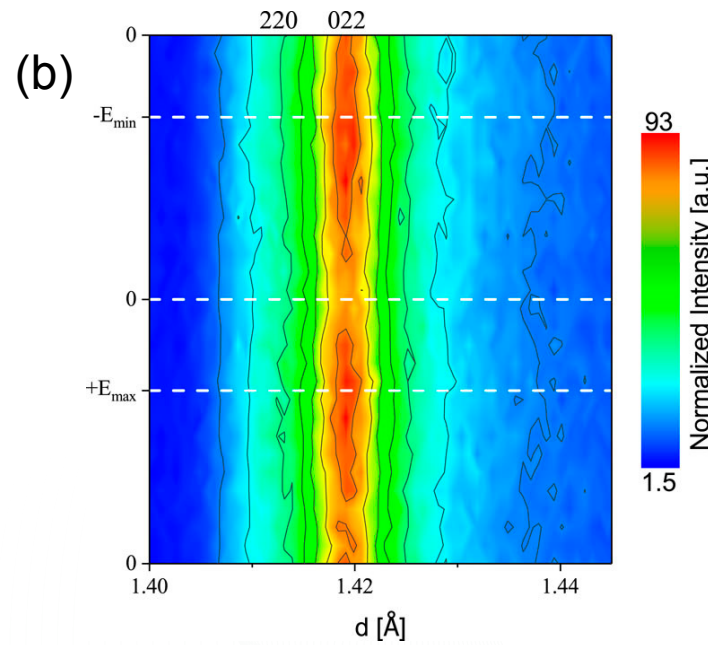
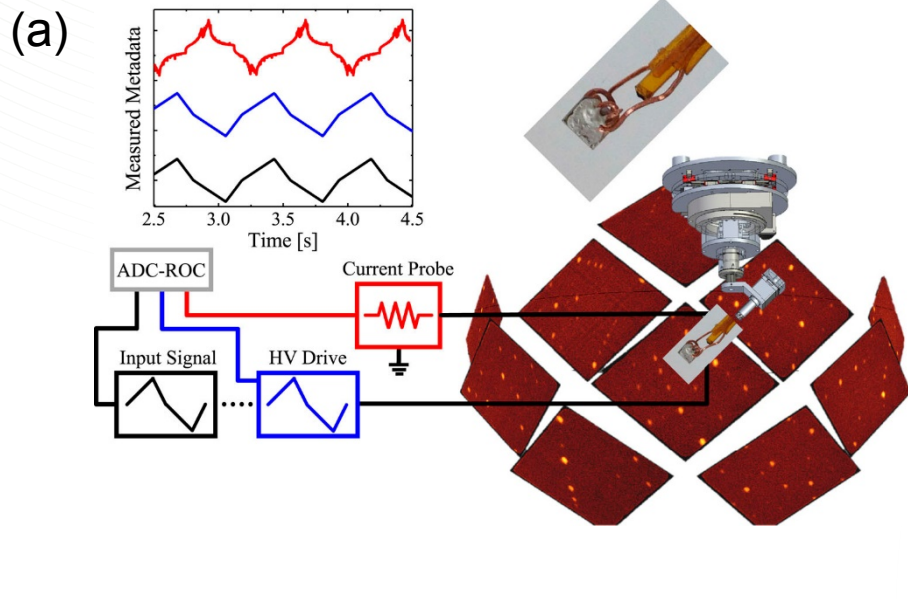
Hoffmann C., Sedov V.N., Parizzi A.,
Zhou W., Schultz A.J., Wang X.P., Long D.

Data Acquisition System at SNS Instruments



SNS Real Time Data Link (RTDL), a 10 MHz, bi-phase mark encoded serial link.
Signals have **100 nanosec.** resolution.

Dynamic structural response

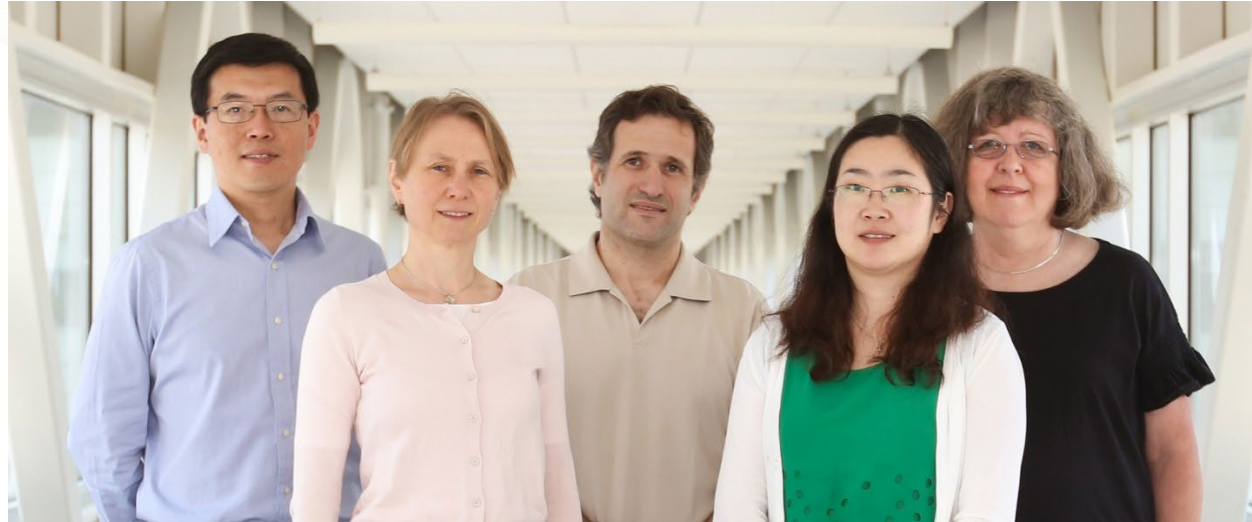


(a) The experimental setup to demonstrate the time-filter methods (b) BaTiO_3 022/220 diffraction evolution during the application of the modified triangular waveform. Maxima in the intensity of the 022 reflections are observed at $\pm E_{\max}$, evidencing ferroelastic DWM.

Perspectives

- Diffraction space
 - Multi-dimensional single crystal diffraction **(3 + n)d**
 - Accurate hydrogen positions in energy materials
 - Modulation wave vectors from local structure variations
 - Superspace approach to solve complex magnetic structures
- Parameter space
 - Time filtering/slicing of neutron TOF Laue data under external stimuli p_i
 - Dynamic field response
 - Hydrogen position and movement of ferroelectric organic molecules
 - Non-equilibrium
 - Optoelectronic responsive hybrid organic-inorganic perovskites
 - 3D diffuse scattering
 - Evolving dynamics of relaxor ferroelectrics with an applied electric field
 - Time-resolved neutron Pair Distribution Functions (t -PDF)

The SNS TOPAZ Team



Xiaoping Wang, Christina Hoffmann, António M. dos Santos, Helen He, Vickie Lynch
Left to right

neutrons.ornl.gov/topaz

The neutron single crystal study at ORNL's Spallation Neutron Source TOPAZ instrument is sponsored by the Scientific User Facilities Division, Office of Basic Energy Sciences, US Department of Energy.

Thank You for your attention!